Evaluating River Profile Geometries to Identify Evidence of Active Deformation Associated with the Doty Fault Zone in Southwest Washington

Varqa Tavangar

A report prepared in partial fulfillment of
the requirements for the degree of

Master of Science
Earth and Space Sciences: Applied Geosciences

University of Washington
June, 2019

Project mentor:
Dr. Lydia Staisch, United States Geological Survey

Reading committee:
Dr. Alison Duvall, University of Washington
Dr. Juliet Crider, University of Washington

MESSAGe Technical Report Number: 076

Executive Summary

In 1996, 2007, and 2009, flooding of the Chehalis River near the Town of Chehalis in southwest Washington severely impacted infrastructure and property. Damage was such that Interstate 5, the major transportation throughway in this region, was closed for several days. In 2012, the Washington State Geological Survey and United States Geological Survey began an assessment of the seismic hazards posed by the regional and local geologic systems on proposed construction of a dam near the Town of Pe Ell, Washington. Of these structural systems, the Doty Fault Zone is of interest as; (1) its level of activity is not well known, (2) its geometry is not described in detail, (3) it extends along a portion of the Chehalis River, and (4) would pose a hazard to the construction of the dam if it were active.

The Doty Uplift (DU) is one of several basement uplifts in southwest Washington, and the western extent of the Doty Fault Zone bounds the southern boundary of the DU. In this report, the morphology of streams draining the DU are studied and characterized to identify topographic evidence of active deformation associated with the Doty Fault Zone. I performed a digital analysis of the morphology of twenty-two streams, including the description of channel steepness and longitudinal-profile geometry and the identification of knickpoints, or locations of sharp changes in the channel slope along each river. The influence of lithology and the discrimination between discrete (fault-related) and persistent (anticlinal and lithologic) forcings were considered in the analysis.

Patterns in the normalized channel steepness index (k_{sn}) across the study site show increasing k_{sn} values moving upstream along drainages within the DU. These range from less than ~150m on the outer margins of the DU to ~400m within it. Anomalous high k_{sn} values that rise to up to 800m point to areas on long profiles that may be identified as knickpoints. Ten knickpoints found within the DU are identified, located between elevations of 137 and 320 meters. They range in size from ~4-meter-deep steps to 36 meter near-vertical drops over distances that range between 6 and 45 meters. Nine of the knickpoints are located at higher elevations that the Doty Fault, yet they do not form similar geometries at similar elevations. In addition, the location of the knickpoints in relation to lithologic boundaries and mass wasting deposits introduces complicating factors that make tying these features to fault-related formation tenuous. Six knickpoints are located within the Crescent Formation, three are located within sedimentary units, and one at a lithologic boundary where streams cross over rocks of variable resistances. The lack of spatial continuity and differences in knickpoint form does not point to the influence of an active Doty Fault.

The spatial patterns of normalized channel steepness indices and knickpoints within and around the DU do not point to discrete, fault-offset related causes. Instead, they are likely the product of the structural signature of the Crescent Formation, accented by the influence of lithologic boundaries and mass-wasting deposits. Further investigations of the adjustment of streams of the Doty Hills, thorough in-channel surveys and wider-scale basin instability analyses would help elucidate the topographic evolution of this area.

Table of Contents

Purpose and Scope

In 1996, 2007, and 2009, flooding of the Chehalis River near the Town of Chehalis in southwest Washington severely impacted infrastructure and property (City of Chehalis, 2017). Damage was such that Interstate 5, the major transportation throughway in this region, was closed for several days (The Chronicle, 2017). In 2012, a task force was assigned to develop flood mitigation measures that would prevent this issue in the future. Of these measures, the construction of a dam was proposed along the Upper Chehalis River near the Town of Pe Ell (Ruckelshaus Center, 2012). The Washington Geological Survey and the United States Geological Survey were among those tasked to assess the seismic hazards posed by the regional and local geologic systems on the construction and longevity of the proposed dam.

This seismic hazard assessment provided a timely opportunity to review original studies of the geologic, seismic, and tectonic nature of this region. Additionally, it allowed for more robust geologic investigations to recharacterize the structural systems of southwest Washington, using updated theories of plate tectonics and modern methods of analysis. Of these structural systems, the Doty Fault Zone (Figure 1) is of interest as (1) its level of activity is not well known, (2) its geometry is not described in detail, (3) it extends along a portion of the Chehalis River, and (4) it would pose a hazard to the construction and longevity of the dam if it were active.

This report focuses on identifying and describing indicators of deformation in the landscape that could be associated with an active Doty Fault Zone. More specifically, through studying the morphology of river longitudinal profiles draining the Doty Uplift (DU), this report presents evidence as to what tectonic forcings may explain the spatial distribution and patterns of stream profile morphologies. Furthermore, this report explores the structural and lithologic controls that the Doty Uplift exert on the rivers and discusses the effects on how discrete forcings from the Doty Fault are recorded in the landscape.

Introduction

Understanding how tectonic activity and climatic influences are expressed in the landscape has been a fascinating and ever-studied topic in the geosciences since the 19th century (Dana, 1856; Lyell, 1875; Molnar and England, 1990). In characterizing the natural and dynamic state of the Earth's surface, many metrics, or measurable features of the landscape, have been identified and used (Burbank and Anderson, 2011). At the center of these metrics is the influence of rivers, as they represent first-order controls on topography (e.g., Wobus et al., 2006; Whipple et al., 2013). As the Earth's surface is affected by tectonic and climatic forces, rivers are among the first natural phenomena to adjust to these new conditions. Bedrock rivers are conduits through which tectonic and climatic signals are transmitted across the topography. Their morphology and erosional dynamics make them important features to study, as they dictate the magnitude of changes in topographic relief produced by these forcings (Whipple and Tucker, 1999; Kirby and Whipple, 2001).

Understanding in what ways, and to what extent, rivers have changed can give a preliminary and sometimes illuminating view of what larger-scale, less-visible processes are occurring, or have occurred.

Tectonic and climatic forcings that drive a response from the bedrock rivers can be spatially well distributed across a landscape (precipitation) or localized along sharp boundaries (uplift along a fault). They can be distributed across a gradient or in a uniform manner (anticlinal folding or isostatic rebound). The duration of the perturbation can be described as discrete, persistent, or cyclic. Discrete forcings such as fault rupture or stream capture transmit an isolated signal or pulse through a system. Persistent forcings such as the development of a tectonic stress regime or fault system drive a system towards a new state of equilibrium. Cyclic forcings are those that oscillate between states of equilibrium based on the period of the forcing and the systems response time (Whipple et al., 2013).

In the field of tectonic geomorphology, longitudinal profiles of bedrock rivers have been studied to identify transient responses to tectonic and climatic forcings (e.g., Cyr et al., 2010; Murphy et al., 2016).

Rivers that have experienced a change in forcing – for example a change in rock uplift rate – adjust to new boundary conditions. A common adjustment is a change in channel slope, beginning nearest to where the forcing was applied, propagating headward through the channel network. These changes in channel slope appear as discrete steps, also known as knickpoints, along river longitudinal profiles. They may also appear as broad convexities along profiles, referred to as knickzones. They both show up as spikes in slope vs. drainage-area plots representing breaks in the power-law scaling (Whipple, 2004). The reaches below a knickpoint or knickzone represent the adjustment of channels to new boundary conditions, with reaches above the knickpoint or knickzone representing the relict channel and boundary conditions. Alternatively to propagating headward, in cases where lithologic units create structural controls on river profiles, knickpoints may be stationary. Additionally, for sediment bulges created by mass-wasting processes, knickpoints or zones may propagate downstream as the bulge is dispersed by the stream's erosive power.

To quantify the changes in profile morphology represented by knickpoints, a short discussion of the graded river profile follows. River channels tend toward concave-up profiles that follow Flint's Law (Flint, 1974):

$$S = k_s A^{-\theta}, \quad (1)$$

where S is channel gradient, A is upstream area, k_s is the channel steepness index, and θ is the concavity index. Channel steepness k_s is a measure of channel slope normalized by the contributing drainage area (Duvall et al., 2004; Wobus et al., 2006). Normalization adjusts for the tendency of channel slopes to decrease downstream and allows the erosive potential to be compared between rivers of different sizes. Studies show that k_s is sensitive to rock uplift rate and erosion rate, while θ is shown to be insensitive to such changes (Whipple and Tucker, 1999; Snyder et al., 2000). However, θ covaries with k_s, and to avoid complications of comparing the k_s of drainage basins or streams with different θ values, a reference concavity (θ_{ref}) is chosen to derive a normalized channel steepness index (k_{sn}) (Wobus et al., 2006). Based on stream power analyses and theoretical studies, θ commonly varies from ~0.3 to 0.7 (Whipple and Tucker,

1999; Kirby and Whipple, 2012), and θ_{ref} is often assumed to be around 0.5, which is what is used in the analyses of this report.

Equation 1 works for drainage areas above a critical threshold, A_{cr} (Montgomery and Foufoula-Georgiou, 1993). This critical threshold area is described as the transition from divergent to convergent slopes. The transition is where hillslope processes (debris flows, landslides, etc.) controlling sediment transport and topographic relief shift to fluvial-dominated processes of sediment transport and generating relief. In slope-area plots it is identified by a break in the power-law scaling, where slope does not change with drainage area. This area is ~10^6 m^2 for this report but has been shown to range between 10^5 and 10^7 m^2 (Cyr et al., 2010). It is important to note that there are drainages in this study that have areas below the lower bounds for A_{cr}, and some caution must be used when interpreting profile morphologies of those drainages.

The variable Chi (χ), and χ-elevation plots are outputs of analyses in this report, and although they are not used they must be briefly addressed. χ is a transformed coordinate with a dimension of length and elevation, developed by Perron and Royden (2013) to reduce topographic noise produced when performing slope-area analyses of river profiles. χ-analysis normalizes river profiles for their drainage area, allowing for the comparison of channel steepness across basins of different sizes. As χ is linearly related to elevation, a channel that incises according to the stream power incision model produces a linear χ-elevation profile. A disturbance along a profile, or knickpoint, can be identified as a step or convexity along the χ-elevation plot.

An additional consideration for this report is the influence of varied lithology on the morphology of river profiles and the complications this presents on their interpretations. Boundaries of lithologic units with different strength properties can control knickpoint location and propagation (Pederson and Tressler, 2012; Lima and Binda, 2013), and appear as false-positive deformation-related knickpoints in the landscape. Careful verification of knickpoint locations, or changes in channel steepness, in relation to lithologic boundaries is key in this analysis.

This report studies and characterizes the morphology of streams draining the Doty Uplift in southwest Washington to identify topographic evidence of active deformation associated with the Doty Fault Zone. The characterization of these streams will revolve around the identification of knickpoints and the description of their geometry along river profiles. Spatial distributions of knickpoints, changes in channel steepness, the influence of lithology, and the discrimination between discrete (fault-related) and persistent (anticlinal and lithologic) forcings is presented.

Study Area

Tectonic Setting

The plate tectonic setting of this region is characterized by northeast-directed oblique convergence of the Juan de Fuca and Gorda plates with the North American plate along the Cascadia subduction zone (Figure 2). Subduction occurs at a northwardly-increasing rate of 30-45 mm yr^{-1} (Wilson, 1993). In addition, a clockwise rotation of the overriding Oregon forearc relative to North America at rate of 0.91°/Myr for the past 16 Myr was inferred from paleomagnetic data (Simpson and Cox, 1977; Wells and Coe, 1985). McCaffrey et al. (2007,

2013) subsequently used GPS data from the past 15 years to determine a rotation rate for the Oregon forearc relative to North America of 0.67°/Myr, suggesting broadly comparable short- and long-term rotation rates for the crust (Wells and McCaffrey, 2013). This implies that geologic structures (e.g., folds and faults) accommodating crustal rotation have been actively doing so for at least 16 Myr. The northern Oregon block deforms the Washington forearc as it is buttressed by the Canadian Coast Mountains, creating a regime of north-south shortening characterized by uplift and transpression (Figure 2). The north-south shortening is accommodated by east-west-trending uplifts and associated thrust/reverse faults that include the Seattle Fault zone (Johnson et al., 1994) and, possibly, the Doty Fault Zone.

Geology – Structure and Stratigraphy

The Doty Uplift, otherwise referred to as Doty Hills, is one of several basement uplifts in southwest Washington that includes the Black Hills and Willapa Hills (Figure 3). The DU has been mapped as a west-verging, north-plunging anticline (Pease and Hoover, 1957) (Figure 4). The DU covers an area of approximately 200 km^2, with a length of ~18 km along its inferred axial plane and an east-west width of ~11 km. The Crescent Formation (Arnold, 1906) forms the core and basement of the DU and reaches a maximum thickness of 1.5 km (Pease and Hoover, 1957). This submarine and subaerial Paleocene to Eocene-aged basalt may have formed by extrusion associated with extension along the margin of North America (Wells et al., 1984; Babcock et al., 1992). Overlying and occasionally interbedded with the basalts of the Crescent Formation is the Eocene-aged McIntosh Formation (Snavely et al., 1951a; Moothart, 1993). This marine sedimentary unit runs along the eastern, and portions of the northern and western margins of the DU. The Skookumchuck Formation (Snavely et al., 1958; Armentrout, 1977) overlies the McIntosh to the east of the DU and is characterized by interbedded shallow-marine and continental facies. On the western side of the DU, Eocene to Oligocene-aged Lincoln Creek Formation (Weaver, 1912; Beikman et al., 1967) unconformably overlies the deep-marine strata of the McIntosh (Moothart,1993). This marine sedimentary unit has a maximum thickness of 1 km (Pease and Hoover, 1957) in this area. Along the western side of the DU, the lower to middle Miocene-aged Astoria Formation (Etherington, 1931) overlies the Lincoln Creek with an angular uniformity. Along the southern part of the DU, the Astoria Formation unconformably overlies the Crescent Formation. Intruding into the Astoria Formation along the western and southern margin of the DU is the middle Miocene Grande Ronde Basalt. This flow, associated with the Columbia River Basalt Group, forms a thin ridge running through the area. Finally, the middle to upper Miocene-aged Montesano Formation (Weaver, 1912) overlies the Astoria Formation along the western and southern portion of this area.

The Doty Fault is mapped as a 32 km-long, east-west trending transpressional reverse fault (Wells and Coe, 1985; Moothart, 1993; Brocher et al., 2017) that dips approximately 65° N (Anderson, 2018). Oblique convergence along the fault accommodates components of shortening and shear, with the north side of the fault moving up relative to the south (Figures 5 and 6). The eastern extent of the fault is splayed and crosses the Chehalis River valley near the town of Chehalis. The western extent of the fault is a single strand and bounds the southern portion of the DU. At the western terminus of the Doty Fault, there is a northward step to a similar east-west trending, high angle dip-slip fault that bounds the northern portion of the DU. Preliminary data

from aeromagnetic and ground magnetic surveying (WGS, 2018) have provided a more detailed understanding of the Doty Fault network, with a proposed blind fault running along the western margin of the DU, following the aforementioned northward step. Goals of this and future work by the WGS near the Doty Fault include further geologic mapping, constraining the fault geometry, understanding the connectivity of active faults in the Washington fore arc in the context of a 3D network, and continued seismic and gravity data collection (Anderson, 2018).

Geomorphology

The DU reaches an elevation of 750 m and is drained by streams on all sides. Streams exhibit radial and dendritic drainage patterns, with headwaters forming at elevations of ~620 meters and reaching 4th and 5th order streams between elevations of 106 meters (along the eastern limb) and 182 meters (along the western limb) (Figure 7). The orientation of the DU and presence of major rivers influence the direction in which the streams flow. For this analysis, the streams are grouped into three general flow directions; (1) East-directed streams that drain to the Chehalis River, (2) West-directed streams draining to the Willapa River, and (3) South-directed streams that also drain to the Chehalis River but initially drain perpendicular to and across the Doty Fault. Twenty-two trunk streams are identified and analyzed in this report, and were chosen based on the criteria that their headwaters form near the drainage divide or axial plane, and drain most of the DU. Drainage areas of these streams range from 4 km^2 to 16 km^2 and are well distributed around the DU. The Doty Hills and surrounding areas are heavily logged, with logging roads scarring the landscape seen in the LiDAR imagery. Small and large Quaternary mass-wasting deposits are scattered about the drainages, with landslides as the dominant mode of wasting (Figure 3), occurring throughout headwater and lower portions of the drainages. Quaternary alluvium deposits are mapped along the lower reaches of main-stream segments (Figure 3).

Methods

This study predominantly uses the functions of TopoToolbox (Schwanghart and Kuhn, 2010; Schwanghart and Scherler, 2014) and the Topographic Analysis Kit (TAK) for TopoToolbox (Forte and Whipple, 2018), both MATLAB-based codes. These codes provide a repository of tools to perform a wide variety of high-level topographic analyses. Focusing more on the stream network analysis tools rather than those concerned with drainage basins, this study utilized a suite of functions to produce: (1) Normalized channel steepness (Batch k_{sn}) maps of the Doty Hills and surrounding areas, (2) Distance vs. k_{sn} stream plots, and (3) Distance vs. elevation longitudinal stream profiles. Through these methods, knickpoints are identified and their dimensions and spatial distributions described. By also looking at their locations in relation to lithologic boundaries, mass-wasting deposits and the mapped location of the Doty Fault, I interpreted potential driving mechanisms for stream profile discontinuities.

First, LiDAR Digital Elevation Models (DEM) of southwest Washington were obtained from the Washington DNR LiDAR Portal (2018) and USGS (2018) and mosaicked together.

Next, the ‘MakeStreams’ tool was used to output the necessary base datasets for use in the following TopoToolbox functions. The mosaicked DEM was used as the input in this function,

and the base datasets that are created include a 'FLOWobj' that stores flow routing information, similar but not entirely like a flow direction raster in ArcGIS. Additionally, a 'GRIDobj' was created to store the gridded raster data, in the form of the DEM and flow accumulation raster.

The 'KsnChiBatch' function was used to create a normalized channel steepness (Batch k_{sn}) map for all channels within the specified reference frame or area. The output was stored as a shapefile and imported into ArcGIS to superimpose on the DEM.

To graphically visualize how normalized channel steepness (k_{sn}) varies along the stream profiles, the 'KsnProfiler' function was used. This produced Chi-Elevation and Distance-Elevation plots for individual streams, but most importantly Distance-k_{sn} plots for each stream. From these plots entire or partial stream segments were chosen to show what the average k_{sn} and changes in k_{sn} were for each stream.

The 'SegmentPicker' function was then used to manually highlight individual streams that meet the criteria of having headwaters near the crest of the Doty Hills, and flow across an entire limb or side of the anticline. These criteria allow for the potential to identify areas of active deformation that may have propagated to any position along the length of the stream. For each chosen stream, the outputs of the 'SegmentPicker' function were Chi-Elevation, Distance-Elevation, and logSlope-logDrainage Area plots. Knickpoints can be identified as steps or convexities in the Chi-Elevation and Distance-Elevation plots, while they show up as spikes along the fluvial portion of the logSlope-logDrainage Area plot.

Subsequently, the streams were plotted based on their general flow direction (East, West, South) using the 'SegmentPlotter' function. In instances where significant differences in outlet elevations made the illustrations difficult, the streams were partitioned and grouped slightly differently. Within this function, one can zoom in to areas of interest along the profiles to identify knickpoints and potentially trace their location along discrete elevation bands. The fault geometry and location and geologic units were then drawn in approximately based on previous geologic mapping.

Results

Large-Scale k_{sn} Patterns

From the Batch k_{sn} map, large-scale patterns can be seen along the drainages, and smaller scale areas of interest can be identified. The Batch k_{sn} map of the study area shows a pattern of increasing normalized channel steepness moving up drainage networks of the DU (Figure 8). Normalized steepness indices on the outer margins of the DU, at lower elevations (less than 200 meters) are generally less than 150m, while the majority of k_{sn} at higher elevations (200 to 620 meters) range between 200 and 400m. Outliers to this pattern within the DU, i.e. stream segments with anomalously high k_{sn} values that match with steps along longitudinal profiles can be identified as knickpoints or knickzones (Figure 9). These k_{sn} values range from 400 to 800m, with an outlier value of 1459m resulting from an artifact of the DEM. When cross-referenced with the geologic units of this area, the k_{sn} values greater than 250m occur almost entirely within the Crescent Formation.

To further explore the larger-scale patterns of k_{sn} values of the DU, I compared the longitudinal profile geometries of individual streams using the KsnProfiler outputs. As mentioned above, the DU streams were grouped into West, East and South sections based on initial flow directions. Figure 10(A-C) graphically represents the distance-k_{sn} plots for chosen streams within each of these groupings. West-directed streams have the lowest k_{sn} with an average of 170m, followed by East-directed streams with an average k_{sn} of 228m, and South-directed streams have the highest average k_{sn} of 254m. This presents a curious pattern where the western limb of the anticline, with steeper dips ranging from 30° to 75°W depending on lithology (Pease and Hoover, 1957), yields streams with lower average k_{sn} than the eastern limb with shallower dips ranging from 20° to 35°E (Pease and Hoover, 1957). This pattern does not show an influence of the proposed blind fault extending along the western limb of the DU. Moreover, the drainages on the western side funnel across outcroppings of Grande Ronde Basalt and Astoria Formation, which may impose structural controls on the development of these basins and help produce the observed patterns of k_{sn}. Interestingly, the south-directed streams that cross the fault have the highest average k_{sn}, and the sharpest k_{sn} changes occur just below and above the Doty Fault. The proximity of the k_{sn} changes to the fault, lithologic boundaries and their elevations will be further explored in the following section.

Small-Scale Knickpoints of Interest

Figure 9 shows the ten knickpoints and knickzones that were identified from the k_{sn} map and longitudinal profiles. Six are located within the Crescent Formation at elevations between 182 and 320 meters and three are located within marine sedimentary units between elevations 137 to 243 (Figure 11). Finally, one is located across multiple lithologies at an elevation of 152 meters. For reference, the Doty Fault crosses the south-directed streams between elevations 158 and 228 meters.

Figure 12 shows a composite of south-directed streams with breaks in slope labeled as knickpoints. These are of varying sizes, with smaller ones (Stream 2 at elevation 182 meters) dropping ~4 meters over a distance of 4.5-6 meters, and larger ones (Streams 4 upstream knickpoint, at elevation 213 meters) with a 34-meter deep step over 45 meters.

The knickpoint identified along Stream 2, located within the Crescent Formation, coincides with a debris flow deposit where the stream is diverted and cuts through the deposited material (Figure 13). Furthermore, convexities or high k_{sn} values seen in the headwater area of Stream 2 can be explained by the mapped mass-wasting deposits in the area (Figure 14). These may be feeding larger caliber sediments into the stream, propagating downward through the drainage as sediment bulges, showing up as high k_{sn} values.

In a similar vein, the knickpoints along streams 4, 5 and 6, when examined in relation to lithologic boundaries and proximity to the fault, have some complicating issues. Figure 15 shows this location of incised reaches that extend from above to below the fault, beginning within the Crescent Formation and deepening as it moves through the Astoria Formation, finally crossing the thin rib of more resistant Grande Ronde basalt. Additionally, the incised reaches are located at the confluence of two tributaries. The interplay between changes in resistance at lithologic

boundaries and an increase in stream power muddles the ability to identify this feature as a fault-related knickpoint.

The Stream 4 upstream knickpoint is one of the largest identified in this area. The lack of other knickpoints of similar size and at similar elevation points to this feature being a product of the Crescent Formations local structure. This may represent a boundary between massive to columnar block-jointed flows where incision has cut down through weaknesses in the rock and then along a lower resistant surface. Additionally, the Stream 6 incised reach shows a related structural signature of the Crescent Formation that creates extensive incised reaches, appearing as steps along stream profiles.

Along the eastern side of the fold, there are four knickpoints identified along the stream profiles (Figure 16). Most striking is the step along Stream 14, dropping 36 meters over 6 meters at an elevation of 243 meters, upstream from the northern fault (Figure 17). This can be classified as an over-steepened reach, or vertical knickpoint. As mentioned previously, the lack of other knickpoints of similar size and at similar elevation suggests this is the product of the Crescent Formation's structure (perhaps transition between flow boundaries). The change in erosional mechanics and effects on knickpoint migration rate (Crosby and Whipple, 2006) that this over-steepened reach introduces is another complicating factor in attributing this knickpoint to fault-related activity.

Along Stream 12, two possible knickpoints are identified. The upstream step drops ~12 meters over ~30 meters, and the downstream step drops 4.5 meters over a distance of 6 meters (Figure 18). The upstream knickpoint coincides with a lithologic boundary, here between the Crescent and McIntosh Formations and perhaps just downstream from an unmapped mass-wasting deposit. The downstream knickpoint is uniquely located solely within the McIntosh Formation, and is the lowest knickpoint identified in this study. Although this stream does not cross the Doty Fault, this feature is ~ 20 meters lower in elevation than the Doty Fault, and if fault-related knickpoints propagate headward through drainages, a knickpoint downstream from this may not be related.

To better visualize the west-directed streams, as there are significant differences in their outlet elevations, they are separated in Figure 19. Just below the confluence of streams 17 and 18, there is a step of ~4 meters over a distance of 21 meters at an elevation of 243 meters (Figure 20). This occurs as the stream flows to the southwest, crossing the boundary of the Lincoln Creek Formation and the Astoria Formation. Stream 21 has a knickpoint that drops ~3 meters over ~30 meters (Figure 21). It is located within the Lincoln Creek Formation, and in an interesting area that has been highly influenced by humans. Logging roads run along this reach and the stream appears to be undercutting the route. Further field inspection must be completed to definitively state what processes are occurring there.

The results presented illustrate the intricacies involved in interpreting tectonic information from topography. Lithologic boundaries and mass-wasting processes are shown here to play key roles in complicating how fault-related knickpoints may be identified in the Doty Hills. The dominant

control on knickpoint form and location is tied to the structure of the Crescent Formation and boundaries with marine sedimentary units, rather than fault-related activity.

Discussion

Regional trends in normalized channel steepness from this analysis constrains high k_{sn} values not only to within the DU (Figure 8) but more so to the Crescent Formation (Figure 9). The structural control that the basalt imposes on the streams and the lack of said control from the sedimentary units can be clearly seen. Streams flowing over more resistant rocks, albeit through streams of lower-order, do not erode and assume a convex form compared to the streams flowing over less resistant rocks.

The three stream groupings of this analysis provides additional insight into the observed patterns of k_{sn}. West-directed streams have the least relief from headwaters to their chosen outlets, and the erosive power required to produce concave profiles would be less than that required by south- and east-directed streams with greater relief. In addition, the steeper dips of the Crescent Formation (30° to 75°W compared to 20° to 35°E along the eastern limb) provides an orientation where the headwater streams have less erosive work to accomplish a concave up profile. No large (greater than 10-meter-deep) knickpoints are identified along this portion, compared to those on the south and east sides (Streams 4 and 14). For the east- and south-directed streams, the most striking knickpoints occur at lithologic boundaries (Streams 4, 5 & 6) and within the Crescent Formation possibly related to basalt flow boundaries or areas of jointing or fracturing where streams preferentially erode.

Gravity anomaly data showing significant vertical offset from the proposed blind fault suggests that this area of the forearc is experiencing or experienced significant east-west shortening on geological time scales (Anderson, 2018). However, the lack of geomorphic evidence of fault activity in the Doty Uplift may show that the southern boundary of the deforming Puget Lowland block has shifted northward.

The scale and geometry of the study area may also be a limiting factor in this analysis. The Doty Fault runs at a high elevation across the south-directed trunk streams, and there is only a short distance over which knickpoints may propagate before the signals are muted by headwater hillslope processes. Debris flows and landslides are shown here to have strong influences on profile geometry and therefore on k_{sn}.

Teasing apart the effects of climatic and tectonic forcings is a difficult task but must be mentioned. The southernmost extent of the Frasier glaciation around 15,000 years ago reached only ~11 km from this area. Although isostatic rebound was negligible (Thorson, 1989), regional effects of base level changes through repeated glaciations may have had a ripple effects that travelled up river networks. The effects of a dramatic base level rise from deglaciation on streams of the Doty Hills has not yet been explored. If the streams were affected, how would it impact how they communicate tectonic signals through their networks?

Field-based studies of this area may shed light on other ways rivers adjust to tectonic and climatic forcings. For example, channel width adjustment has been shown to occur in areas of

variable lithology experiencing similar tectonic stresses. Additionally, a study of the sediment character and hillslope inputs along these streams would improve the interpretations made on their morphology. Looking larger-scale to basin metrics, there could be important information to learn from the stability of Doty Hills drainage basins. Additionally, a comparison of the geomorphology and k_{sn} patterns of other basement uplifts such as the Willapa and Black Hills could help explain the results of this report.

Conclusion

This report presents the characterization of twenty-two streams and the identification and description of knickpoints along river profiles. The descriptions are in the context of their spatial relationships, geometries, changes in normalized channel steepness (k_{sn}), and the influence of lithologic boundaries and mass-wasting deposits. Normalized channel steepness indices patterns of this area show increasing k_{sn} values moving upstream along drainages within the Doty Uplift. These range from less than ~150m on the outer margins of the Doty Uplift to ~400m within it. Anomalously high k_{sn} values that rise to up to 800m point to areas on long profiles that may be identified as knickpoints. Ten knickpoints found within the DU are identified, located between elevations of 137 and 320 meters. They range in size from ~4-meter-deep steps to 36 meter near-vertical drops over distances that range between 6 and 45 meters. Nine of the knickpoints are located at higher elevations that the Doty Fault, yet they do not form similar geometries at similar elevations. In addition, the location of the knickpoints in relation to lithologic boundaries and mass wasting deposits introduces complicating factors that make tying these features to fault-related formation tenuous. Six knickpoints are located within the Crescent Formation, three are located within sedimentary units, and one at a lithologic boundary where streams cross over rocks of variable resistances. The lack of spatial continuity and differences in knickpoint form does not point to the influence of an active Doty Fault. The spatial patterns of normalized channel steepness indices and knickpoints within and around the Doty Uplift do not point to discrete, fault-offset related causes. They more so are a product of the structural attitude of the Crescent Formation, accented by the influence of lithologic boundaries and mass-wasting deposits. Further investigations of the adjustment of streams of the Doty Hills, thorough in-channel surveys and wider-scale basin stability analyses would help elucidate the topographic evolution of this area.

References

Anderson, M., Lau T., von Dassow W., Reedy T., Staisch L., Cakir R., Sadowski1 A., Polenz M., Becerra R., Toth C., Steely A., Walsh T., Norman D., Sherrod B., 2018. The Doty Fault Network: 3D regional deformation applied to seismic hazard characterization in the forearc of Washington State, American Geophysical Union, Poster T13I-0356.

Armentrout, 3. M., 1977. Cenozoic stratigraphy of southwestern Washington, in Brown, E. FL, and Ellis, R. C., eds., Geological Excursions in the Pacific Northwest: Geological Society of America 1977 Annual Meeting, p. 227-264.

Arnold, R., 1906. Geological reconnaissance of the coast of the Olympic Peninsula, Washington. Bulletin of the Geological Society of America, 17(1), pp.451-468.

Beikman, H. M., Rau, W. W., and Wagner, H. C., 1967. The Lincoln Creek Formation, Grays Harbor basin, southwestern Washington: United States Geological Survey Bulletin 1244-I, p. 11-114.

Brocher, T. M., R. E. Wells, A. P. Lamb, and C. S. Weaver, 2017. Evidence for distributed clockwise rotation of the crust in the northwestern United States from fault geometries and focal mechanisms, Tectonics, 36, 787–818, doi:10.1002/2016TC004223.

Burbank, D.W. and Anderson, R.S., 2011. Tectonic Geomorphology. John Wiley & Sons.

City of Chehalis, 2017. *Flood Information for the Chehalis River Basin*. Accessed 05/27/2019. https://www.ci.chehalis.wa.us/building/flood-information-chehalis-river-basin.

Crosby, B.T. and Whipple, K.X., 2006. Knickpoint initiation and distribution within fluvial networks: 236 waterfalls in the Waipaoa River, North Island, New Zealand. Geomorphology, 82(1-2), pp.16-38.

Cyr, A.J., Granger, D.E., Olivetti, V. and Molin, P., 2010. Quantifying rock uplift rates using channel steepness and cosmogenic nuclide–determined erosion rates: Examples from northern and southern Italy. Lithosphere, 2(3), pp.188-198.

Czajkowski, J. L., Bowman, J. D., 2014. Faults and earthquakes in Washington State, Washington Division of Geology and Earth Resources Open File Report 2014-05.

Dana, J.D., 1856. On American Geological History. Ezekiel Hayes.

Duvall, A., Kirby, E. and Burbank, D., 2004. Tectonic and lithologic controls on bedrock channel profiles and processes in coastal California. Journal of Geophysical Research: Earth Surface, 109(F3).

Etherington, T.J., 1931. Stratigraphy and fauna of the Astoria Miocene of southwest Washington. University of California Publications, Bulletin of the Department of the Geological Sciences, 20(5), pp.31-142.

Flint, J. J., 1974. Stream gradient as a function of order, magnitude, and discharge, Water Resour. Res., 10(5), 969–973, doi: 10.1029/WR010i005p00969.

Forte, A. M. and Whipple, K. X., 2018. Short communication: The Topographic Analysis Kit (TAK) for TopoToolbox, Earth Surface Dynamics Discussions, p 1-9, https://www.earth-surf-dynam-discuss.net/esurf-2018-57/, doi: 10.5194/esurf-2018-57.

Johnson, S. Y., Potter, C. J., and Armentrout, J. M., 1994. Origin and evolution of the Seattle basin and Seattle fault: Geology, v. 22, p. 71–74, insert.

Kirby, E. and Whipple, K., 2001. Quantifying differential rock-uplift rates via stream profile analysis, Geology, 29, 415–418, doi:10.1130/0091-7613(2001)029<0415:qdrurv>2.0.co;2.

Kirby, E., and Whipple, K.X, 2012. Expression of active tectonics in erosional landscapes: Journal of Structural Geology, v. 44, p. 54–75.

Lima, A.G. and Binda, A.L., 2013. Lithologic and structural controls on fluvial knickzones in basalts of the Parana Basin, Brazil. Journal of South American Earth Sciences, 48, pp.262-270.

Lyell, C., 1875. Principles of Geology Or the Modern Changes of the Earth and Its Inhabitants Considered as Illustrative of Geology: Vol. I and II. Murray.

McCaffrey, R., Qamar, A. I., King, R. W., Wells, R., Khazaradze, G., Williams, C. A., Stevens, C. W., Vollick, J. J., Zwick, P.C., 2007. Fault locking, block rotation and crustal deformation in the Pacific Northwest, Geophysical Journal International, 169, p.1315-1340.

McCaffrey, R., King, R. W., Payne, S. J., Lancaster, M., 2013. Active tectonics of the northwestern U.S. inferred from GPS-Derived surface velocities, Journal of Geophysical Research, 118(2), p. 709-723.

Molnar, P. and England, P., 1990. Late Cenozoic uplift of mountain ranges and global climate change: chicken or egg? Nature, 346(6279), pp.29-34.

Montgomery, D.R. and Foufoula-Georgiou, E., 1993. Channel network source representation using digital elevation models. Water Resources Research, 29(12), pp.3925-3934.

Moothart, S. R., 1993. Geology of the middle and upper Eocene McIntosh Formation and adjacent volcanic and sedimentary rock units, Willapa Hills, Pacific County, southwest Washington (Doctoral dissertation).

Murphy, B. P., Johnson, J. P. L., Gasparini, N. M., and Sklar, L. S., 2016. Chemical weathering as a mechanism for the climatic control of bedrock river incision, Nature, 532, 223–227, doi:10.1038/nature17449.

Pease Jr, M.H. and Hoover, L., 1957. Geology of the Doty-Minot Peak area, Washington (No. 188).

Pederson, J.L. and Tressler, C., 2012. Colorado River long-profile metrics, knickzones and their meaning. Earth and Planetary Science Letters, 345, pp.171-179.

Perron, J. T., and Royden, L., 2013. An integral approach to bedrock river profile analysis, Earth Surf. Processes Landforms, 38, 570– 576, doi:10.1002/esp.3302

Ruckelshaus Center, 2012. Chehalis basin flood hazard mitigation alternatives report. Washington State University, 532 pp. http://ruckelshauscenter.wsu.edu/wp-content/uploads/2013/06/chehalis-report-12-19-12.pdf.

Schwanghart W., and Kuhn N. J., 2010. TopoToolbox: A set of Matlab functions for topographic analysis. Environmental Modelling and Software, 25(6):770–781. ISSN 13648152. doi: 10.1016/j.envsoft.2009.12.002.

Schwanghart W., Scherler D., 2014. Short Communication: TopoToolbox 2 - MATLAB based software for topographic analysis and modeling in Earth surface sciences. Earth Surface Dynamics, 2:1–7. doi: 10.5194/esurf-2-1-2014.

Simpson, R. W., and A. Cox, 1977. Paleomagnetic evidence for tectonic rotation of the Oregon Coast Range, Geology, 5, 585–589.

Snavely, P.D., Jr., Rau, W.W., Hoover Jr, L. and Roberts, A.E., 1951a. McIntosh formation, Centralia-Chehalis coal district, Washington. AAPG Bulletin, 35(5), pp.1052-1061.

Snavely, P. D., Jr., Brown, R. D., Jr., Roberts, A. E., and Rau, W. W., 1958. Geology and coal resources of the Centralia-Chehalis district, Washington: United States Geological Survey, Bulletin 1053.

Snyder, N., Whipple, K., Tucker, G., and Merritts, D., 2000. Landscape response to tectonic forcing: DEM analysis of stream profiles in the Mendocino triple junction region, northern California: Geological Society of America Bulletin, v. 112, no. 8, p. 1250–1263, doi: 10.1130/0016- 7606(2000)112<1250:LRTTFD>2.3.CO;2.

The Chronicle, '10 Years After 2007 Disaster, Approach to Flooding More Collaborative Than Ever, Leaders Say', Published 12/01/2017.

Thorson, R.M., 1989. Glacio-isostatic response of the Puget Sound area, Washington. Geological Society of America Bulletin, 101(9), pp.1163-1174.

Washington Department of Natural Resources LiDAR Portal, 2018. http://lidarportal.dnr.wa.gov/

Weaver, C.E., 1912. A preliminary report on the Tertiary paleontology of western Washington. Bulletin of the Washington Geological Survey, 15, pp.5-80.

Weaver, C.E., 1937. Tertiary stratigraphy of western Washington and northwestern Oregon, Vol. 3, No. 1. University of Washington.

Wells, R. E., 1984. Paleomagnetic constraints on the interpretation of early Cenozoic Pacific Northwest paleogeography, in Nilsen, T. H., ed., Geology of the upper Cretaceous Hombrook Formation, Oregon and California: Pacific Section Society of Economic Paleontologists and Mineralogists, v. 42, p. 23 1-237.

Wells, R. E., and R. S. Coe, 1985. Paleomagnetism and geology of Eocene volcanic rocks of southwest Washington, Implications for mechanisms of tectonic rotation. J. Geophys. Res., 90(B2), 1925–1947, doi:10.1029/JB090iB02p01925.

Whipple, K. X. and Tucker, G. E., 1999. Dynamics of the stream power river incision model: Implications for height limits of mountain ranges, landscape response timescales, and research needs, J. Geophys. Res.-Sol. Ea., 104, 17661–17674, doi:10.1029/1999jb900120.

Whipple, K.X., 2004. Bedrock rivers and the geomorphology of active orogens. Annu. Rev. Earth Planet. Sci., 32, pp.151-185.

Whipple, K.X., DiBiase, R.A. and Crosby, B.T., 2013. Bedrock rivers. In Treatise on geomorphology. Elsevier Inc..

Wobus, C., Whipple, K. X., Kirby, E., Snyder, N., Johnson, J., Spyropolou, K., Crosby, B., and Sheehan, D., 2006. Tectonics from topography: Procedures, promise, and pitfalls, Geol. S. Am. S., 398, 55–74, doi:10.1130/2006.2398(04).

Figures

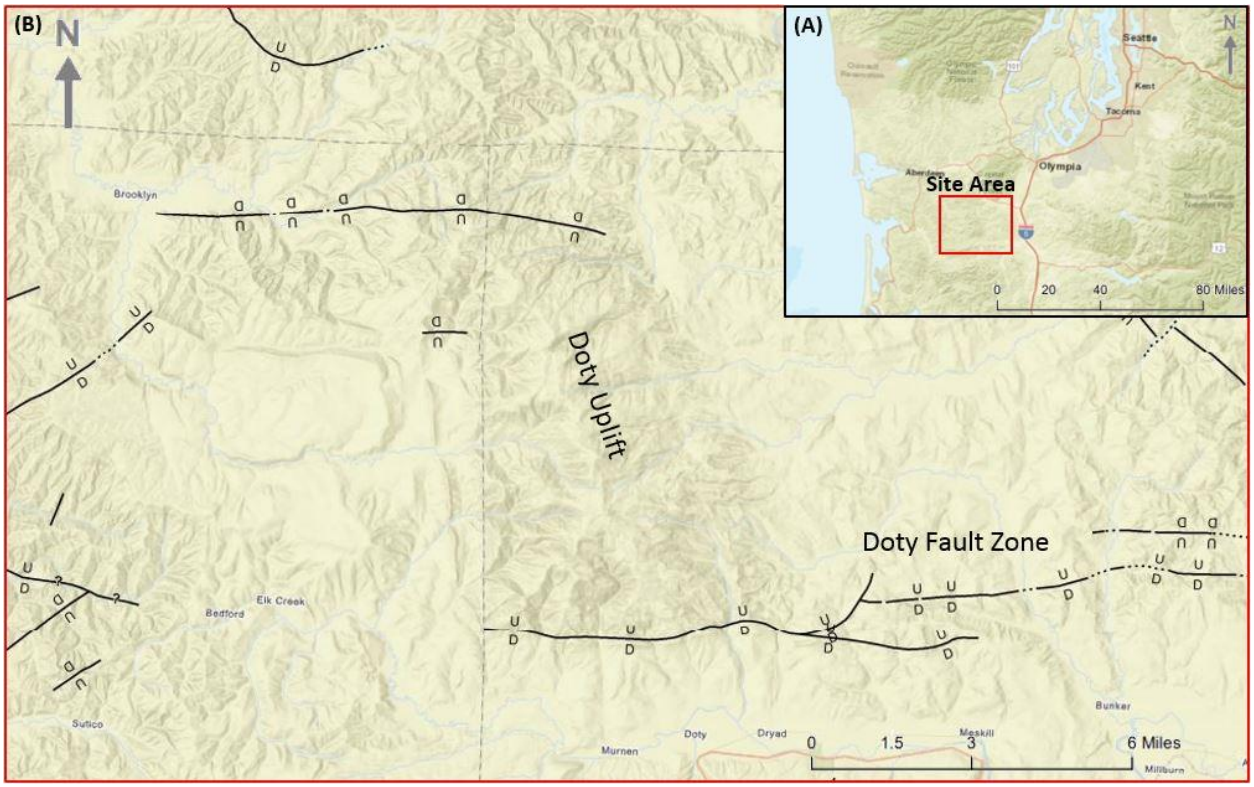

Figure 1. Doty Fault Zone and Doty Uplift located in southwest Washington. Images acquired from WA DNR Geologic Information Portal, 2018. https://geologyportal.dnr.wa.gov/

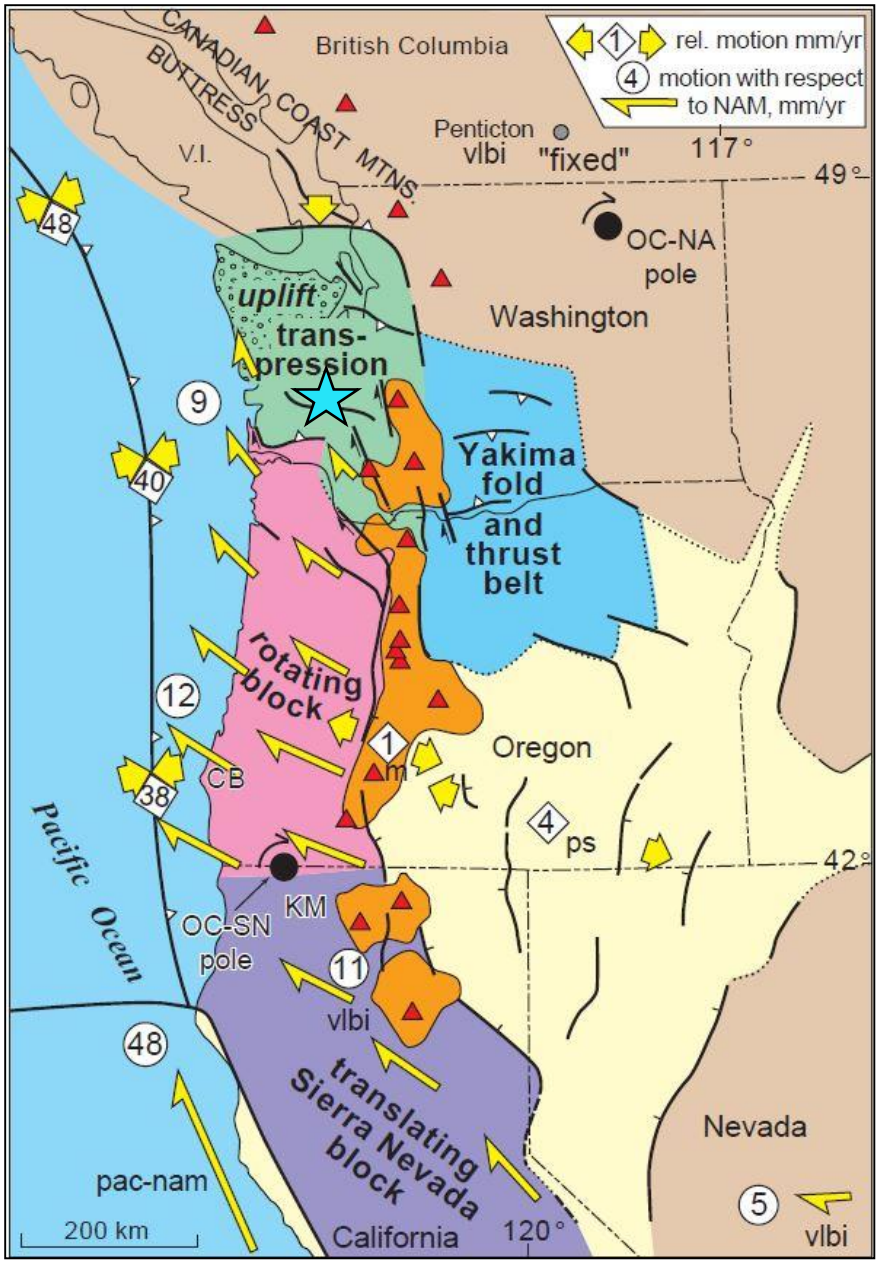

Figure 2. Block rotation for the Pacific Northwest from Wells et al., 1998. The pink Oregon block rotates about the OC-NA pole. Rotational motions are constrained by long baseline interferometry, paleoseismology, magmatic spreading and Pacific-North America motions. Bright blue star is the area of interest.

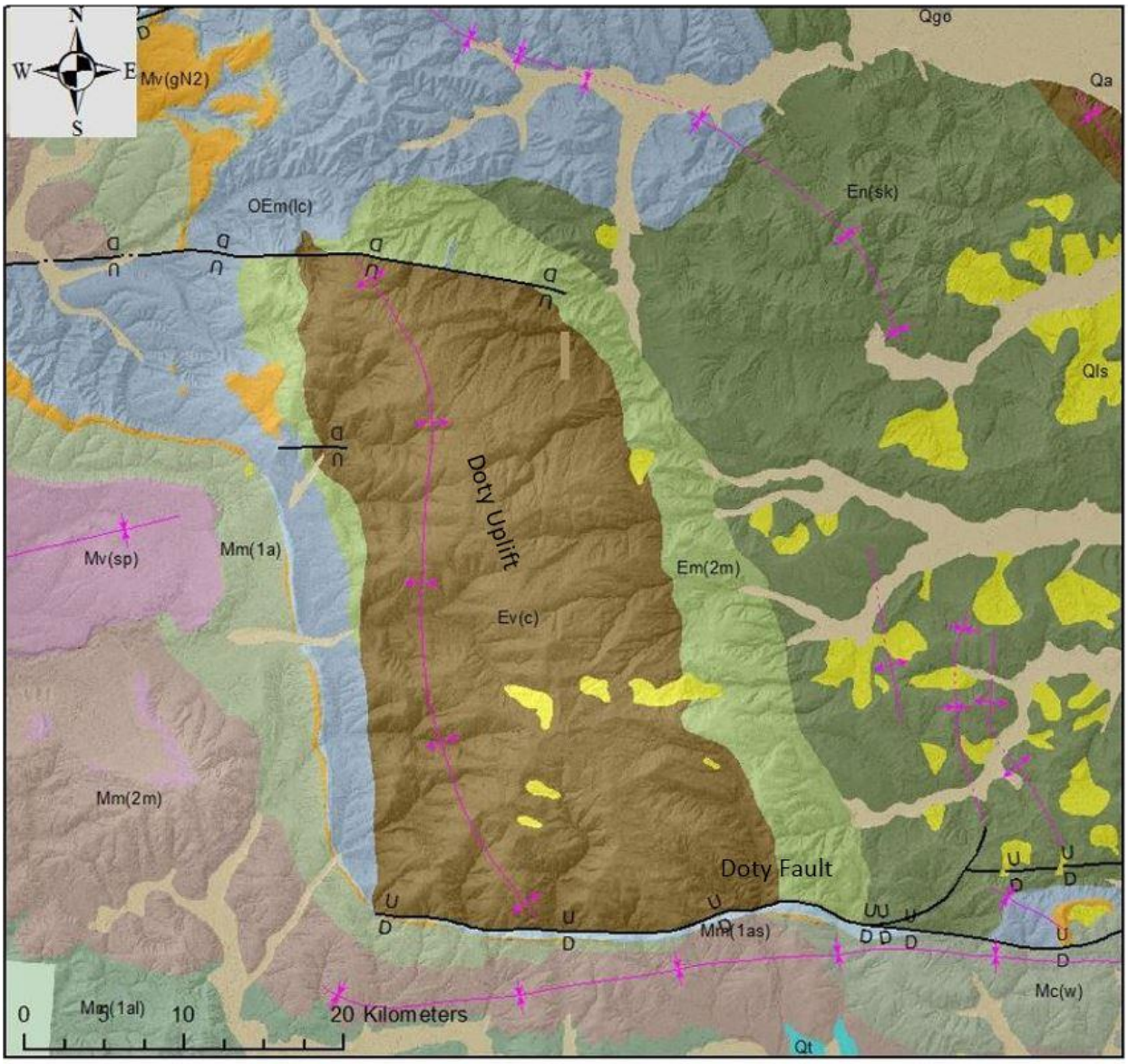

Legend

Geologic Units 100K

Geologic Unit Label

- Em(2m) - McIntosh Formation
- En(sk) - Skookumchuck Formation
- Ev(c) - Crescent Formation
- Mc(w) - Wilkes Formation
- Mm(1a) - Astoria Formation
- Mm(1al) - Astoria Formation – Luisian
- Mm(1ar) - Astoria Formation – Relizian
- Mm(1as) - Astoria Formation – Saucesian
- Mm(2m) - Montesano Formation
- Mv(gN2) - Grande Ronde Basalt – N2
- Mv(sp) - Saddle Mountain Basalt – Pomona
- OEm(lc) - Lincoln Creek Formation
- Qa - Quaternary Alluvium
- Qgo - Glacial Outwash
- Qls - Quaternary Mass-wasting – Landslides
- Qt - Quaternary Terrace Deposit

Figure 3. Geologic Map of the study area created using ArcGIS. Faults (thick black lines) and folds (pink lines and arrows) are also shown.

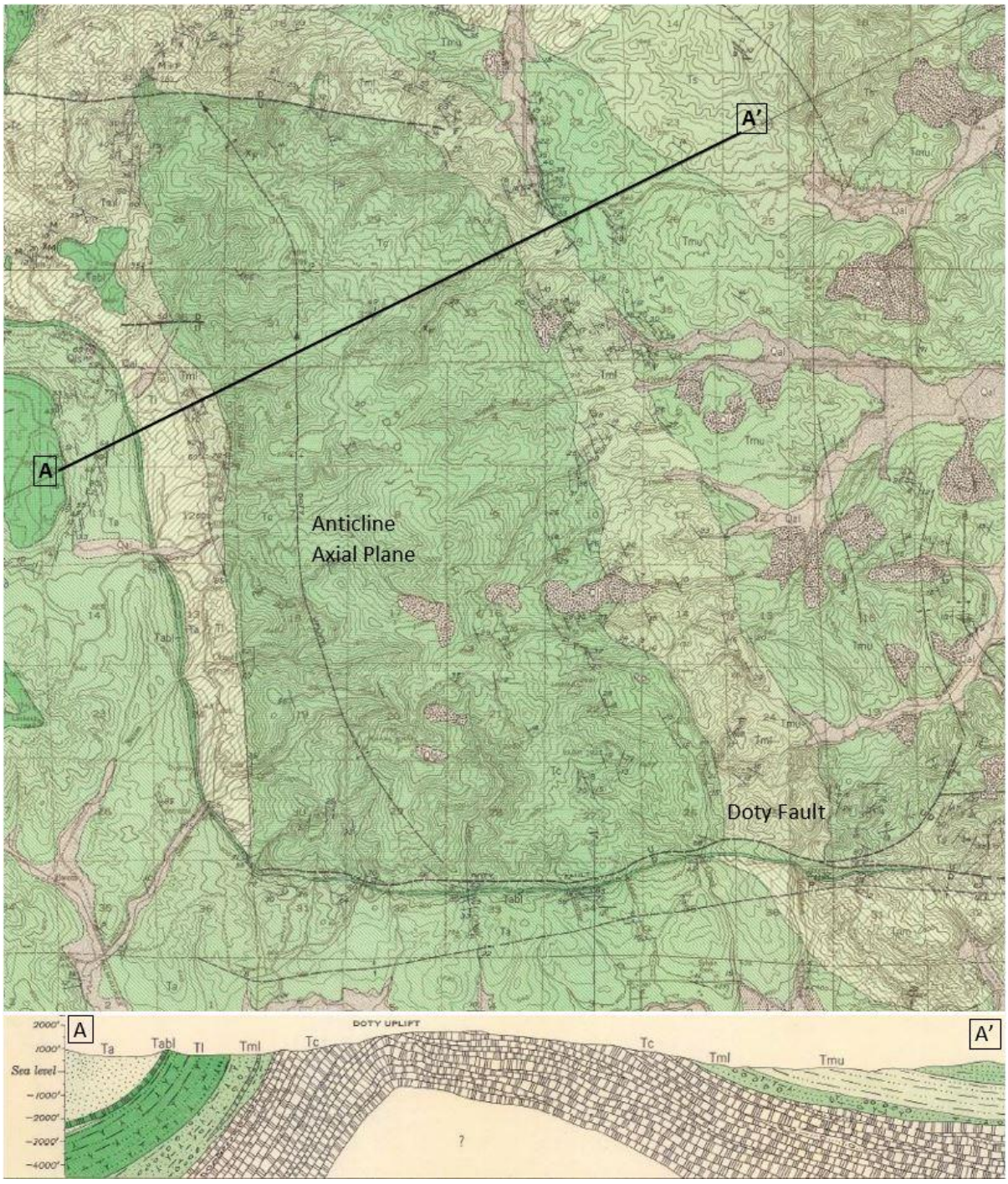

Figure 4. Geologic map and cross section (A-A') of the Doty Anticline from Pease and Hoover (1957). Tc = Crescent Formation, Tml = McIntosh Formation – Lower member, Tmu = McIntosh Formation – Upper Member, Ts = Skookumchuck Formation, Tl = Lincoln Formation, Tabl = Astoria Formation – Lower Member, Ta = Astoria Formation. Contour interval 40 and 80 feet.

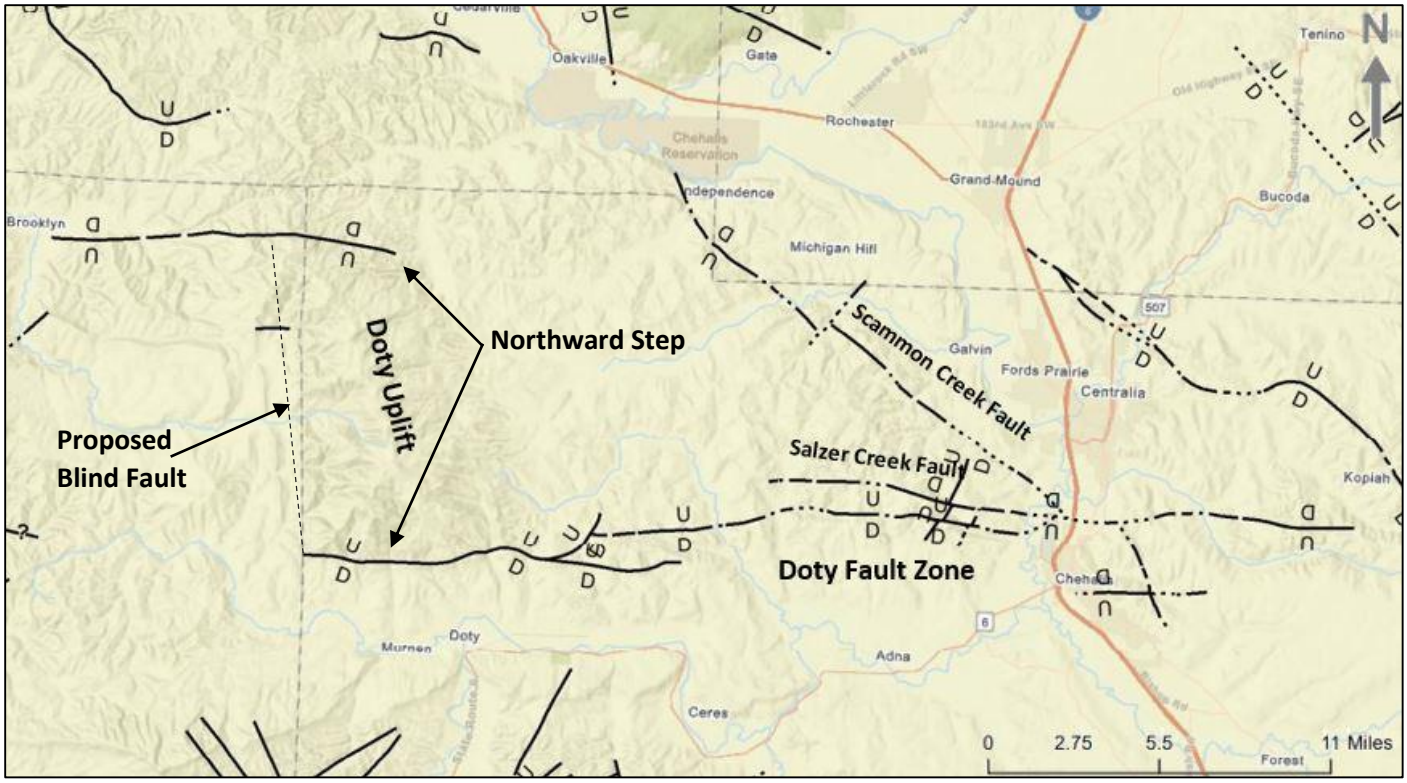

Figure 5. Map showing the northward step at the western terminus of the Doty Fault Zone, with the approximate location of the blind fault proposed by Anderson (2018). Image acquired from WA DNR Geologic Information Portal, 2018. https://geologyportal.dnr.wa.gov/

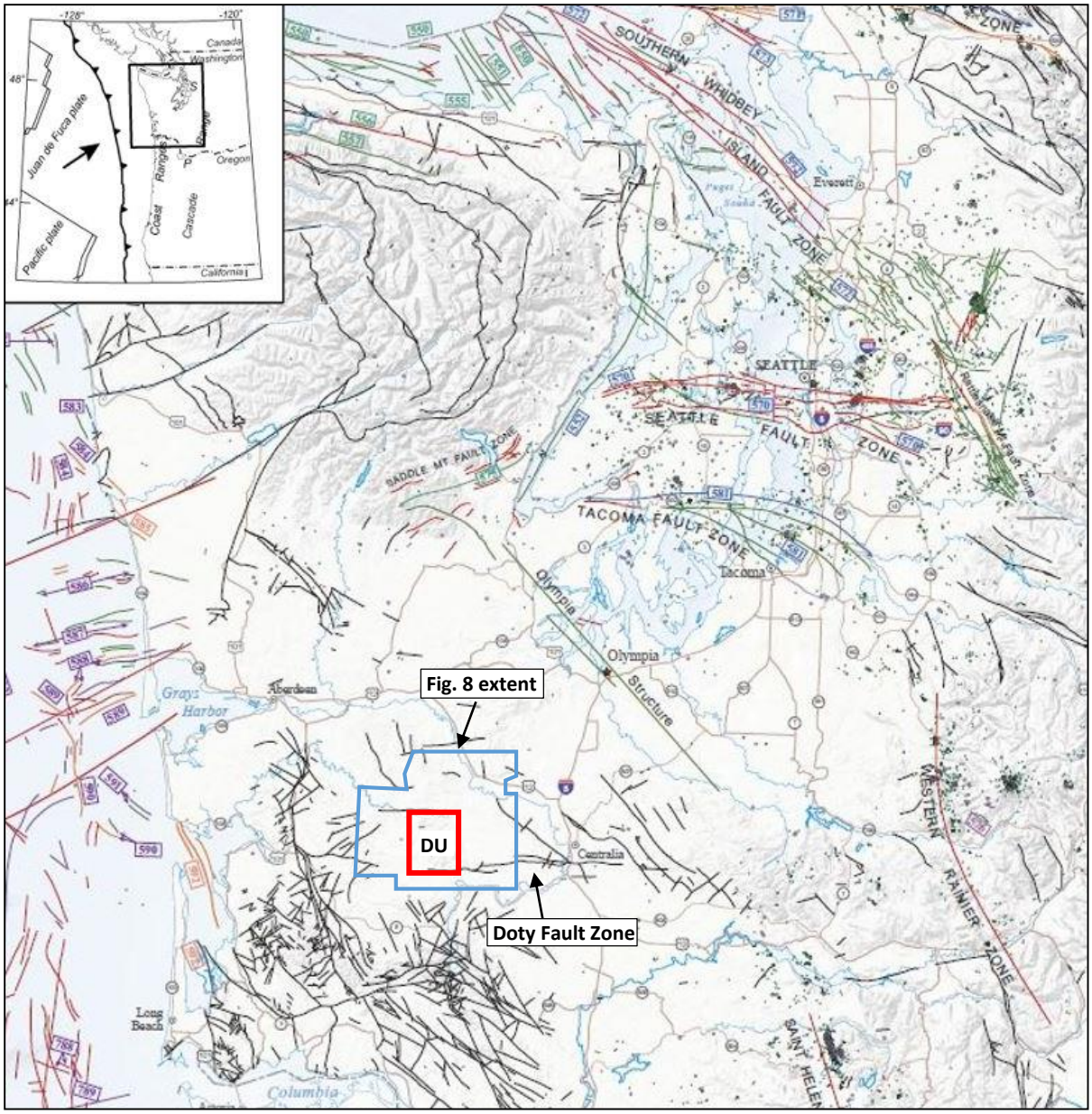

Figure 6. Active fault map for western Washington state (Czajkowski and Bowman, 2014). Green faults show signs of pre-Quaternary activity and purple/blue/orange/red faults show evidence of Pleistocene and later seismic activity.

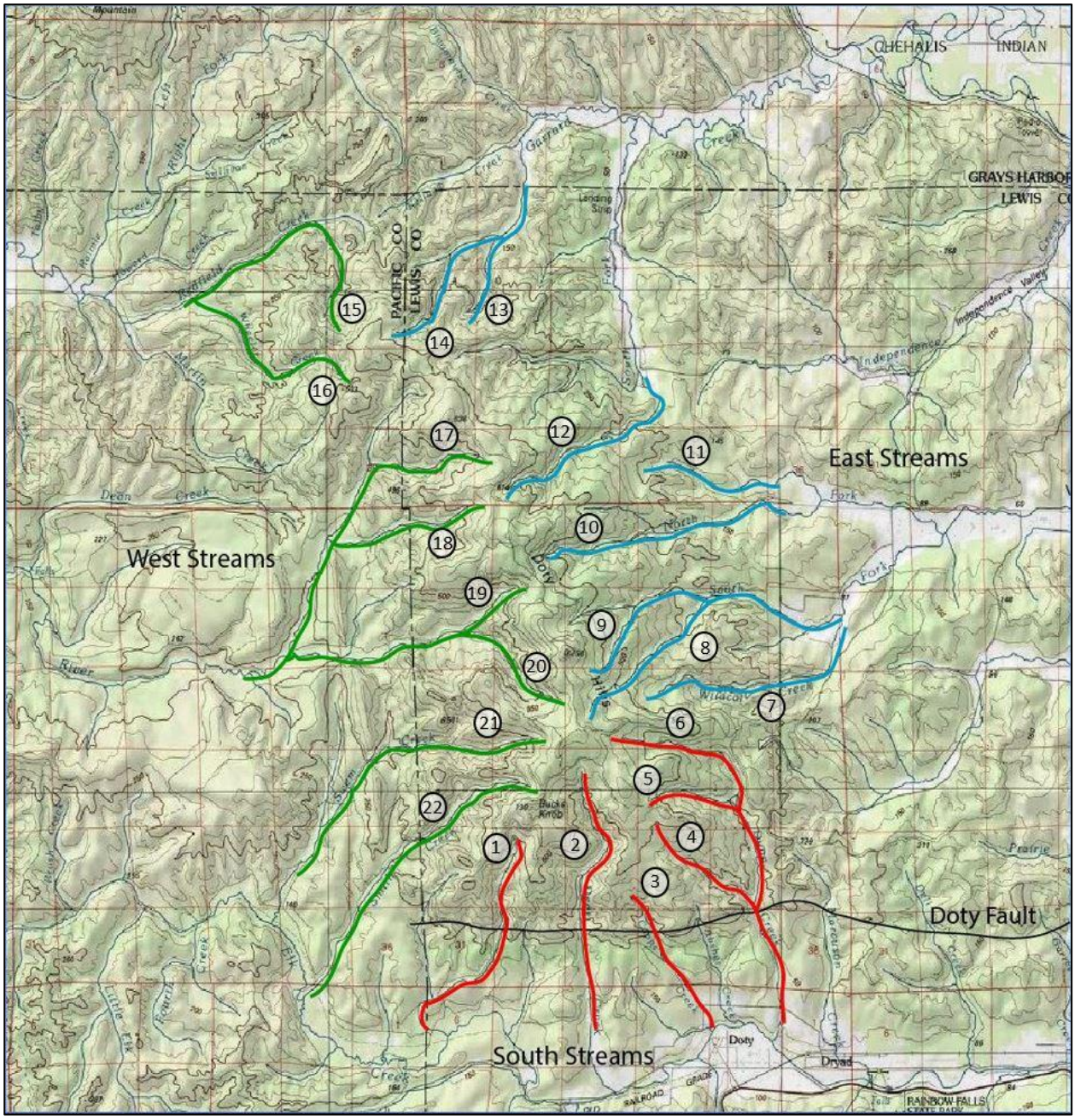

Figure 7. Twenty-two trunk streams are identified in this report. They are grouped into three general flow directions; (1) East-directed streams (2) West-directed streams, and (3) South-directed streams. Image acquired from USGS, 2018. https://ngmdb.usgs.gov/topoview

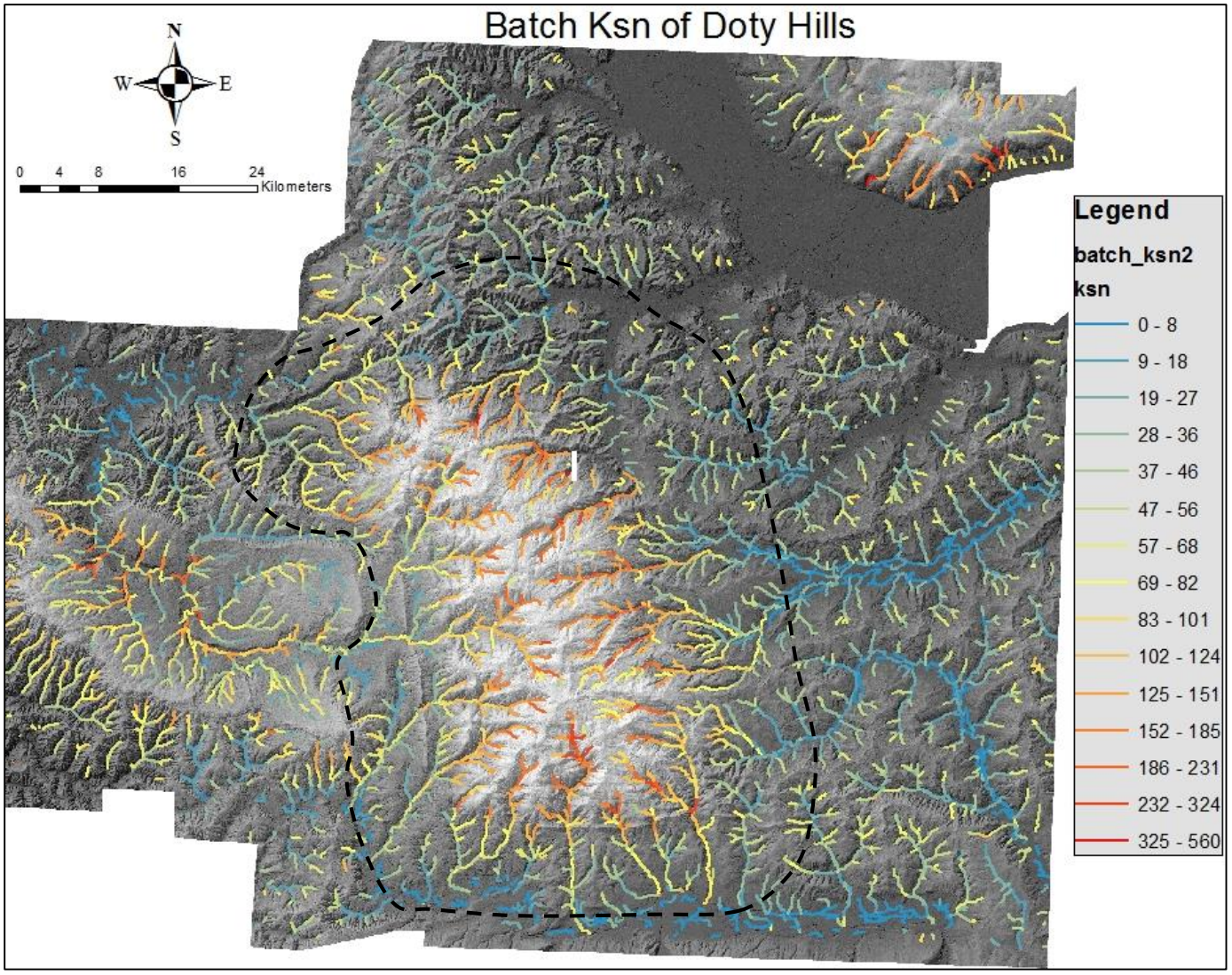

Figure 8. Batch k_{sn} of the Doty Hills and surrounding areas. High k_{sn} values are focused within the DU, with decreasing values shown lower in the drainages. Black dashed line is the approximate extent of the Doty Anticline.

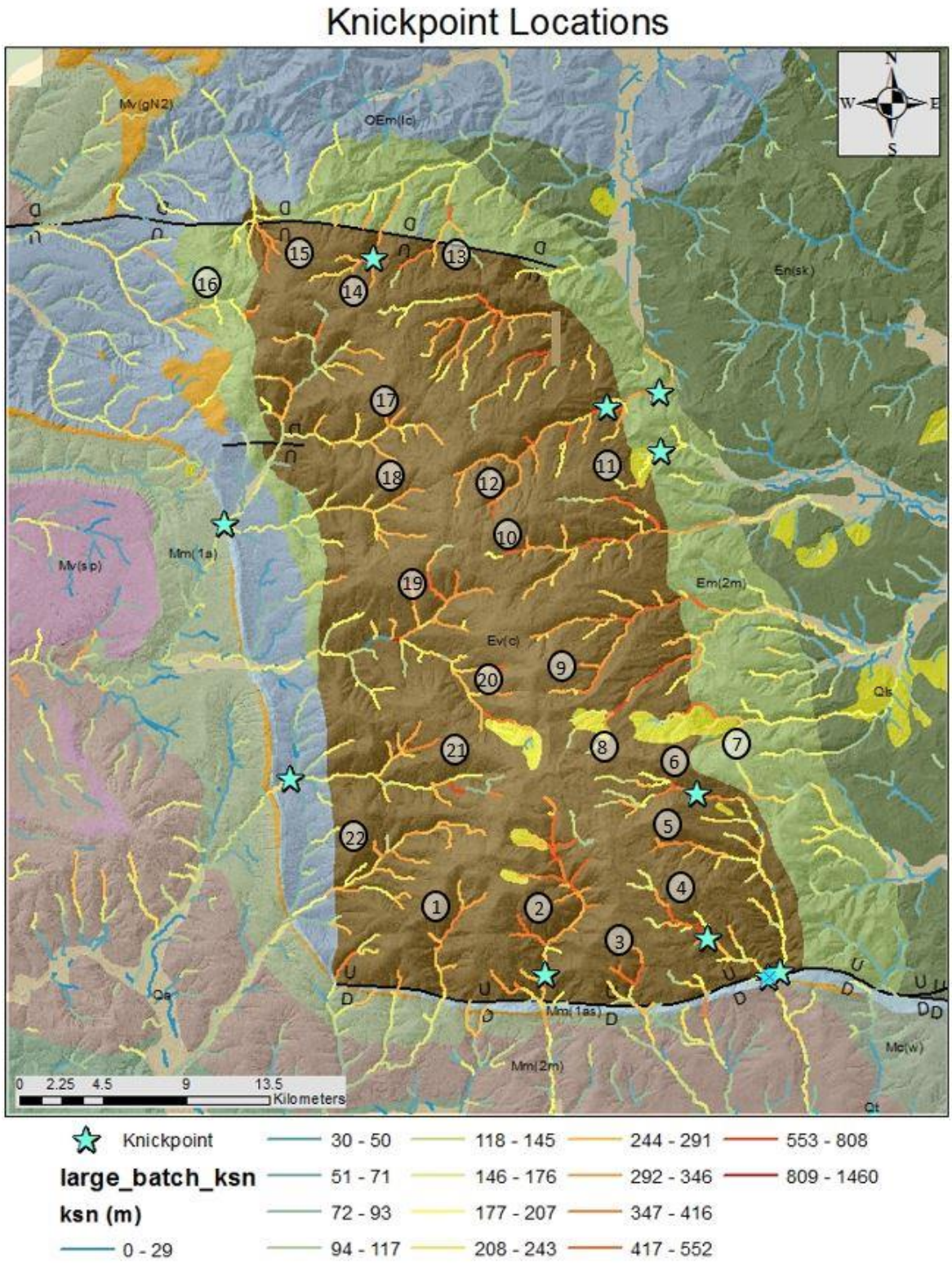

Figure 9. Location of knickpoints identified by sharp changes in k_{sn} values and steps along longitudinal profiles (stars). The highest k_{sn} values are dominantly located within the Crescent Formation. Circled numbers are the streams ID numbers. Thick black lines are faults with their relative motion described as up (U) or down (D).

West Side K_{sn} Profiles

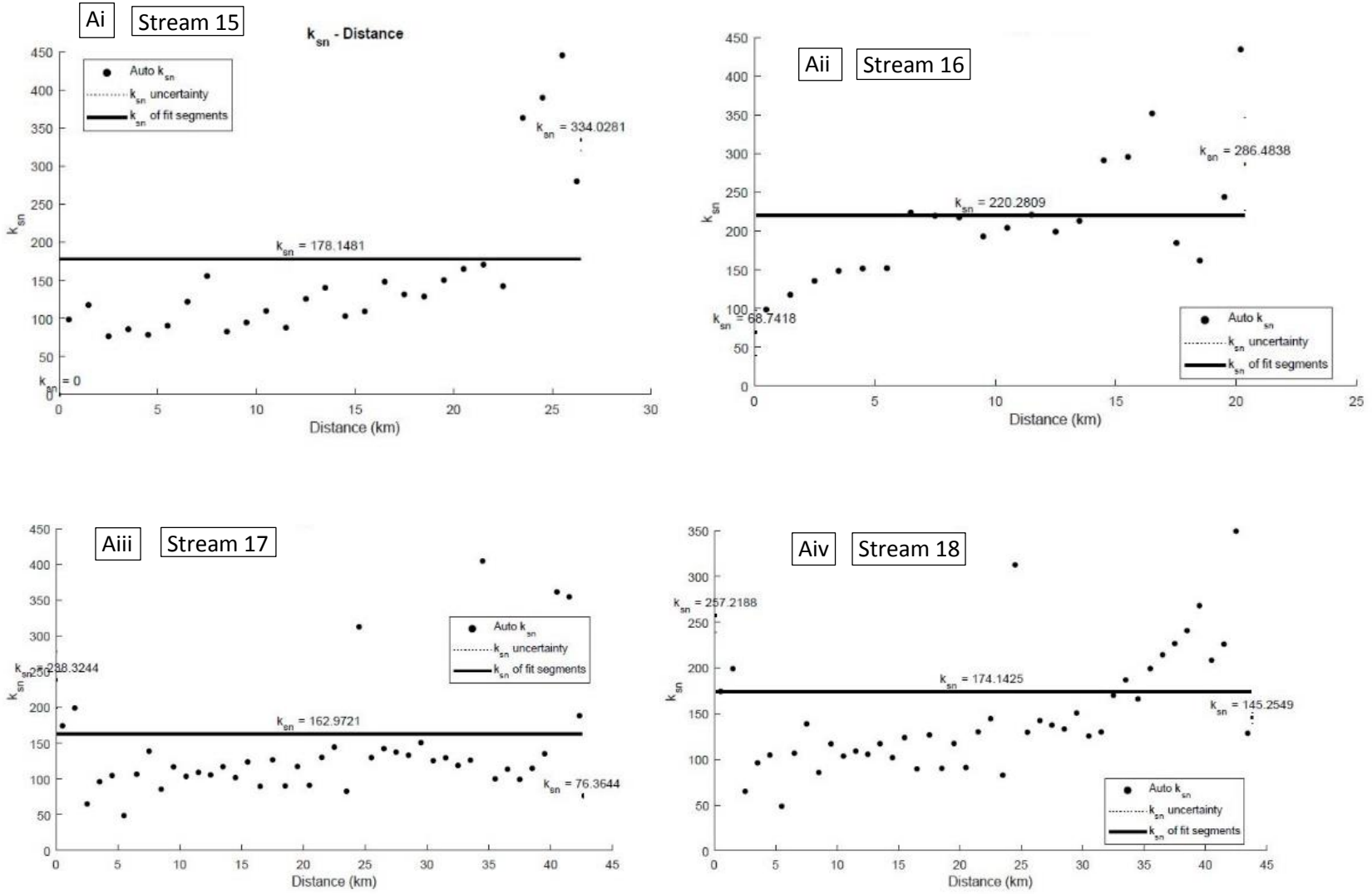

Figure 10 (Ai-Aiv). Outputs of the K_{sn}Profiler function showing k_{sn}-distance plots for west-directed streams 15 through 18.

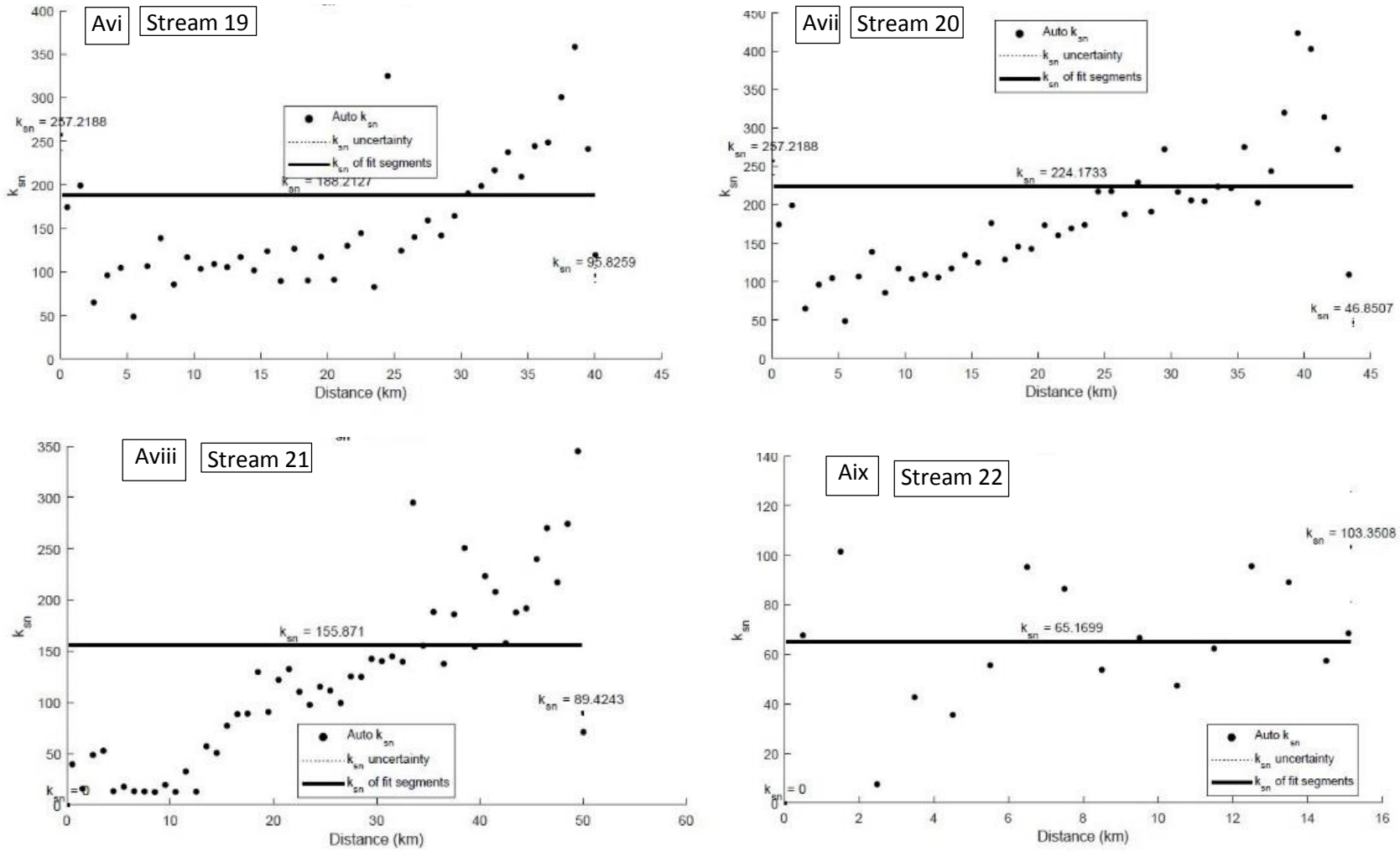

Figure 10 Cont'd (Av-Aix). Continuation of k_{sn} profiles for west-directed streams 19 through 22.

East Side K_{sn} Profiles

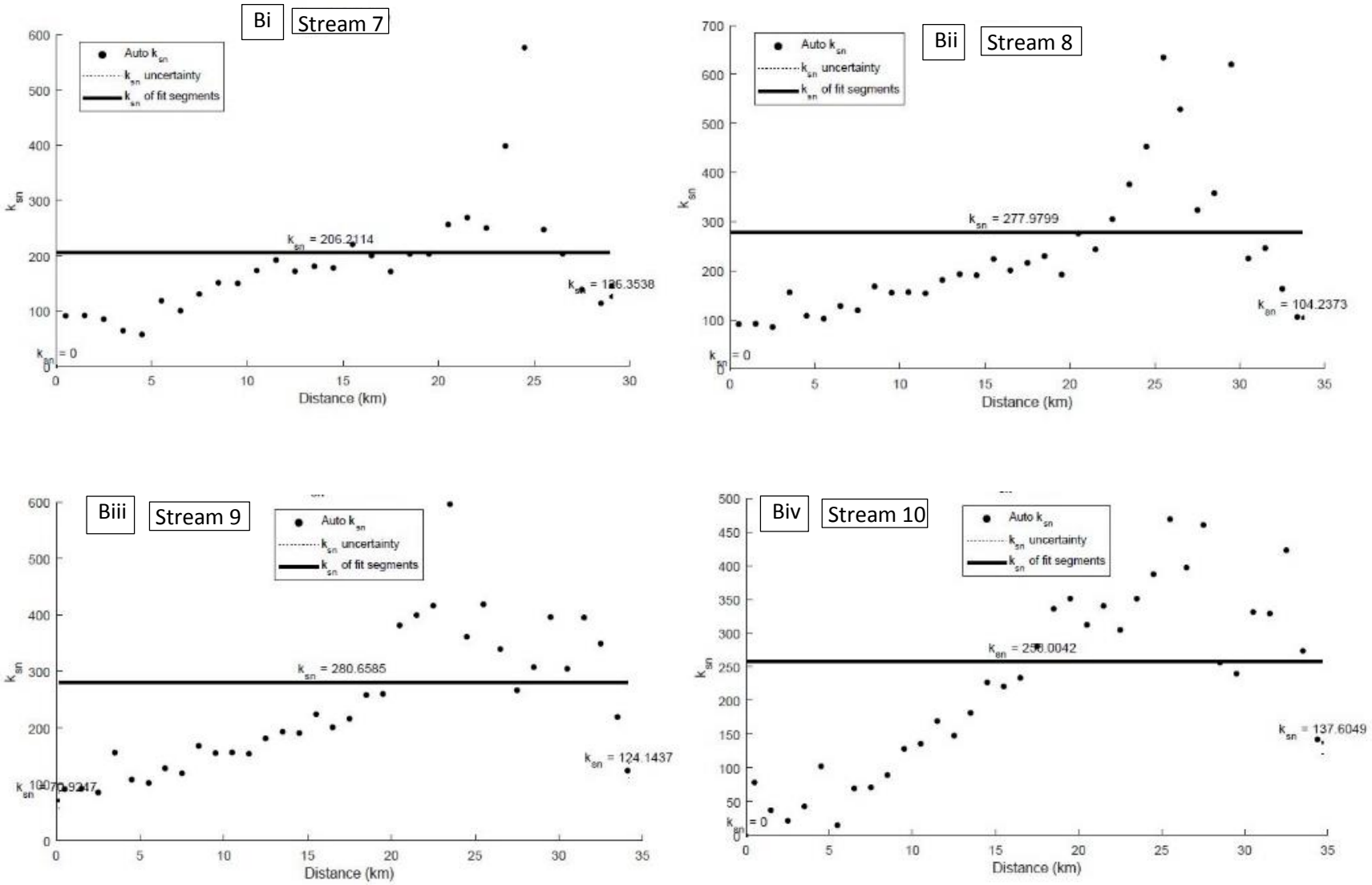

Figure 10 Cont'd (Bi-Biv). Outputs of the K_{sn}Profiler function showing k_{sn}-distance plots for east-directed streams 7 through 10.

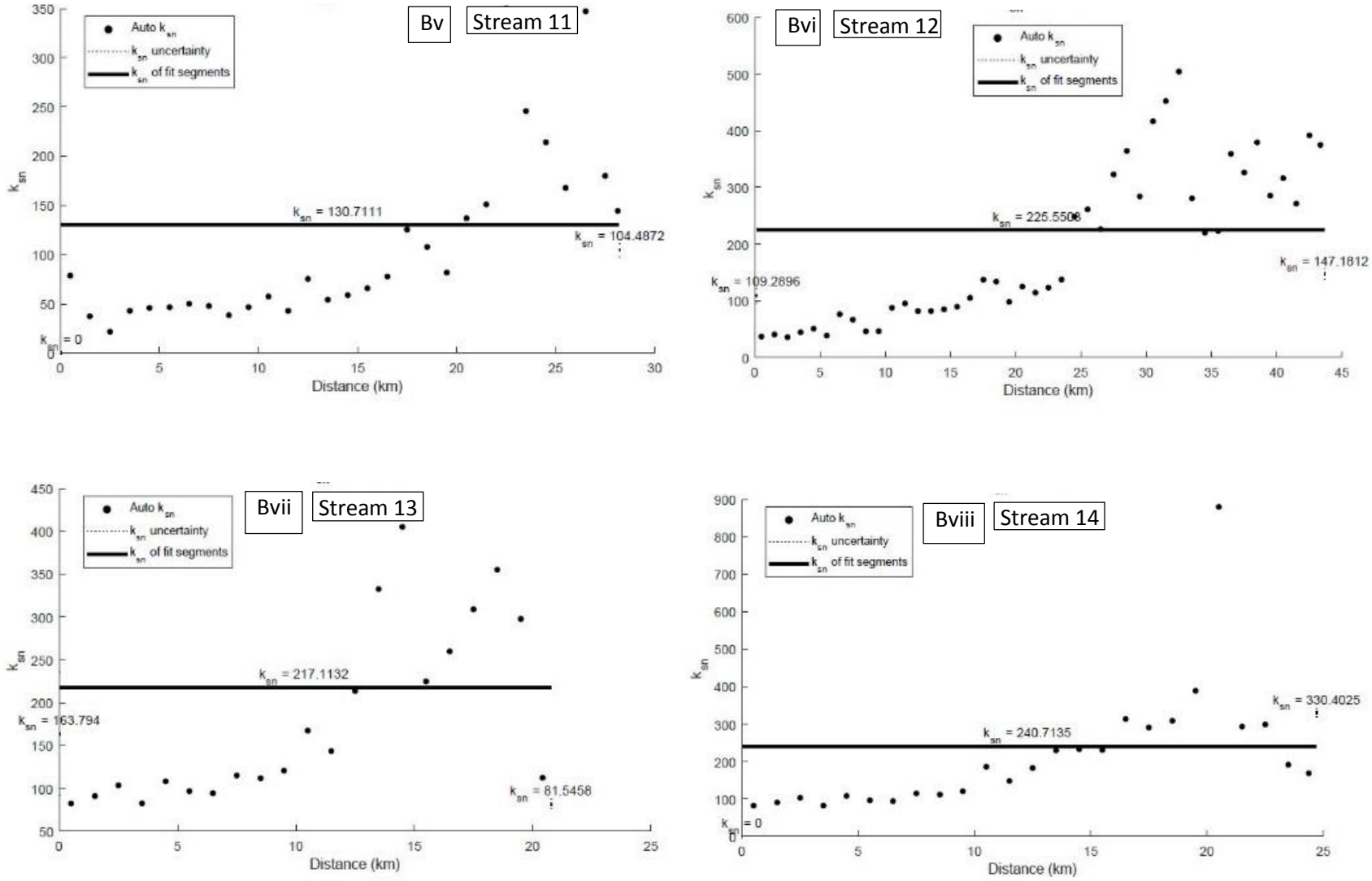

Figure 10 Cont'd (Bv-Bviii). Continuation of k_{sn} profiles for east-directed *streams 11 through 14.*

South Side K_{sn} Profiles

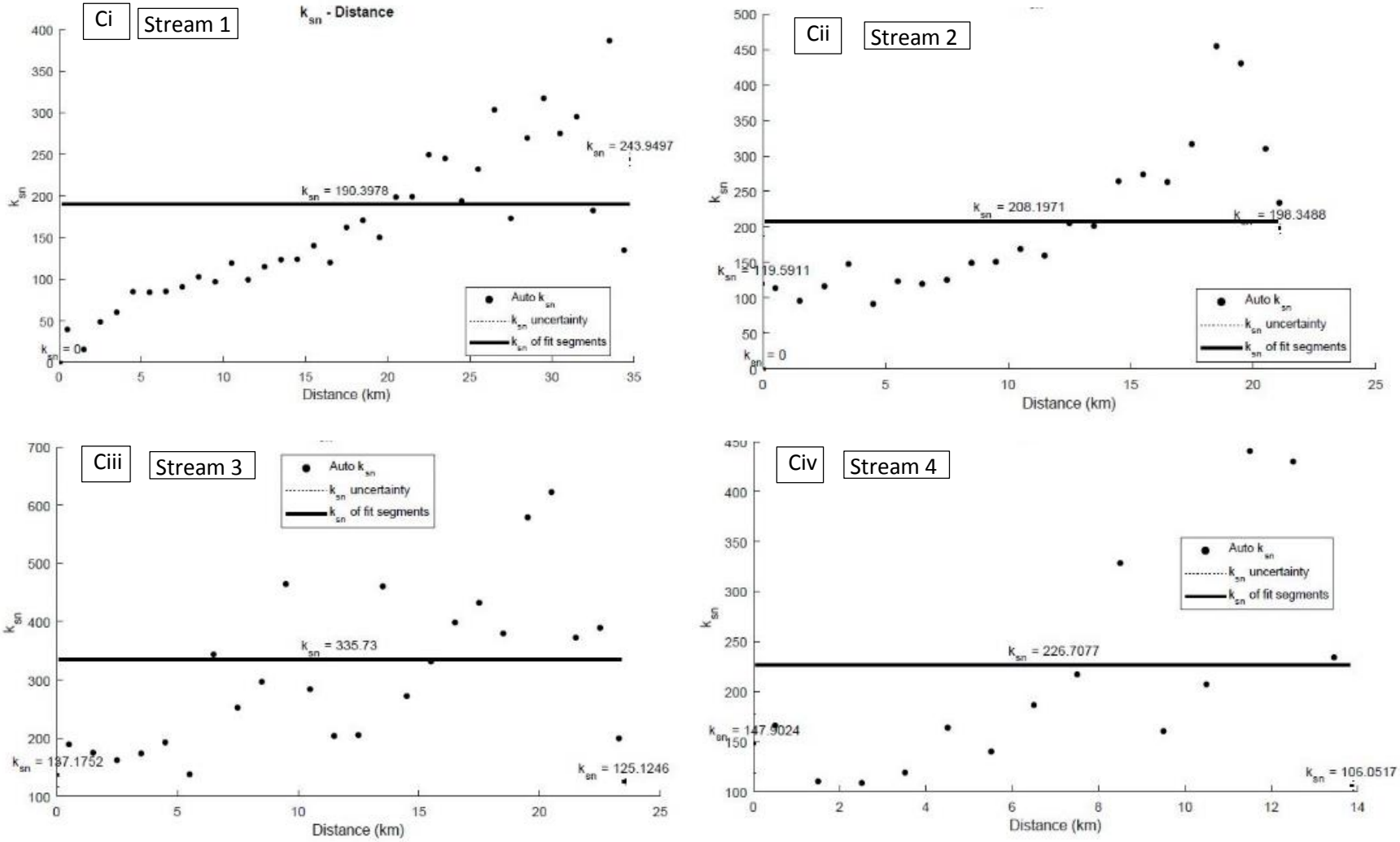

Figure 10 Cont'd (Ci-Civ). Outputs of the K_{sn}Profiler function showing k_{sn}-distance plots for south-directed streams 1 through 4.

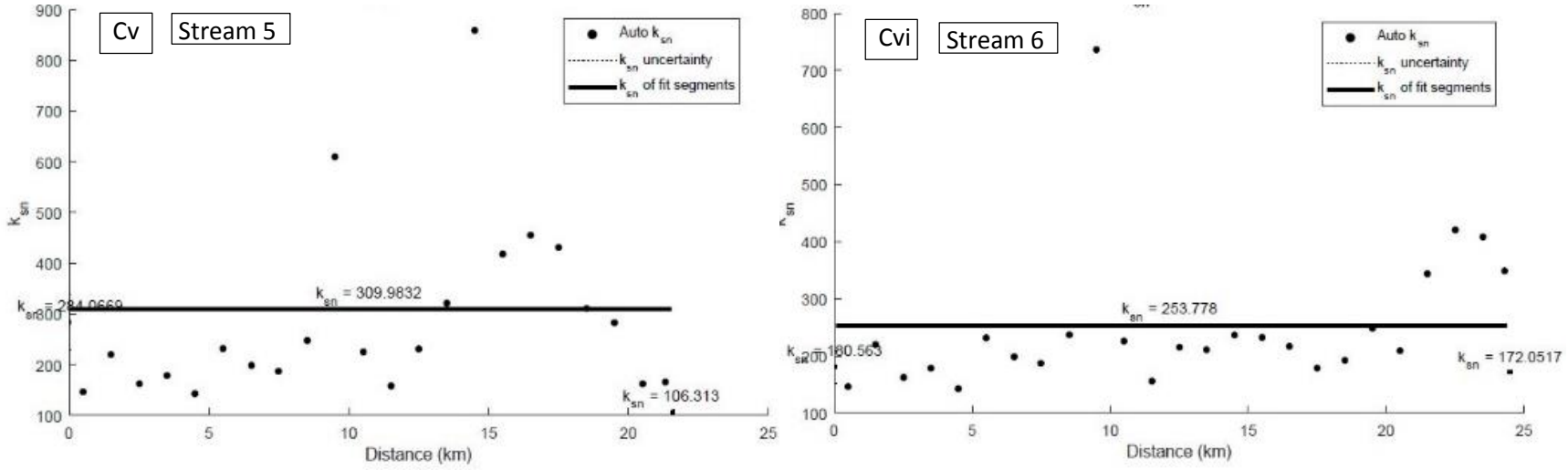

Figure 10 Cont'd (Cv-Cvi). Continuation of ksn profiles for south-directed for streams 5 and 6.

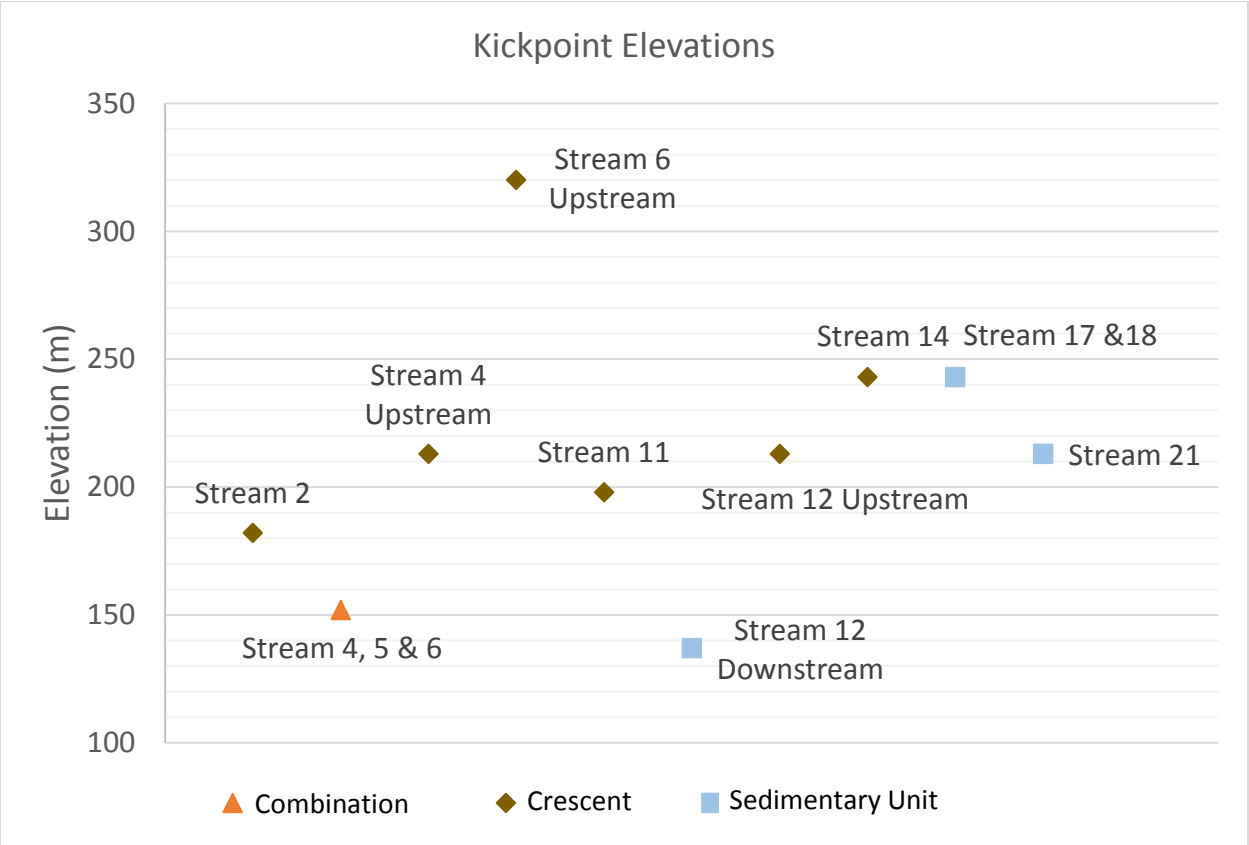

Figure 11. Distribution of identified knickpoint elevations. Diamond symbol indicates knickpoint located within the Crescent Formation. Square symbol indicates a location in marine sedimentary unit. Triangle symbol indicates a combination of both sedimentary and basalt units.

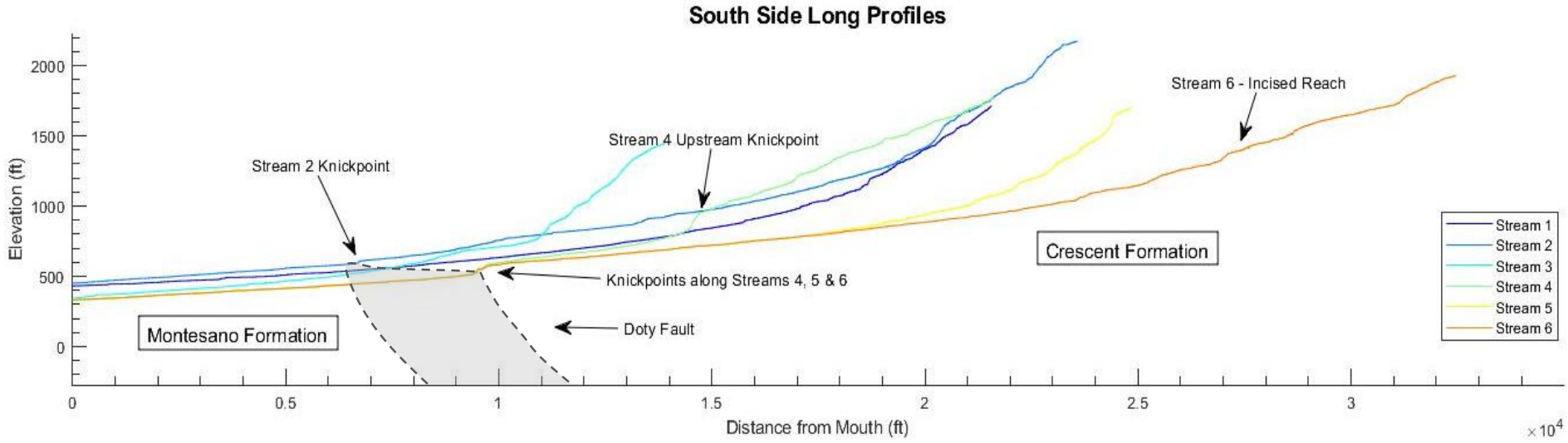

Figure 12. Composite diagram of south-directed stream profiles. The knickpoints and areas of interest along these profiles are highlighted, with the approximate location of the Doty Fault illustrated. The fault line here is also used an approximate location of lithologic boundaries (Crescent-Astoria-Grande Ronde-Montesano).

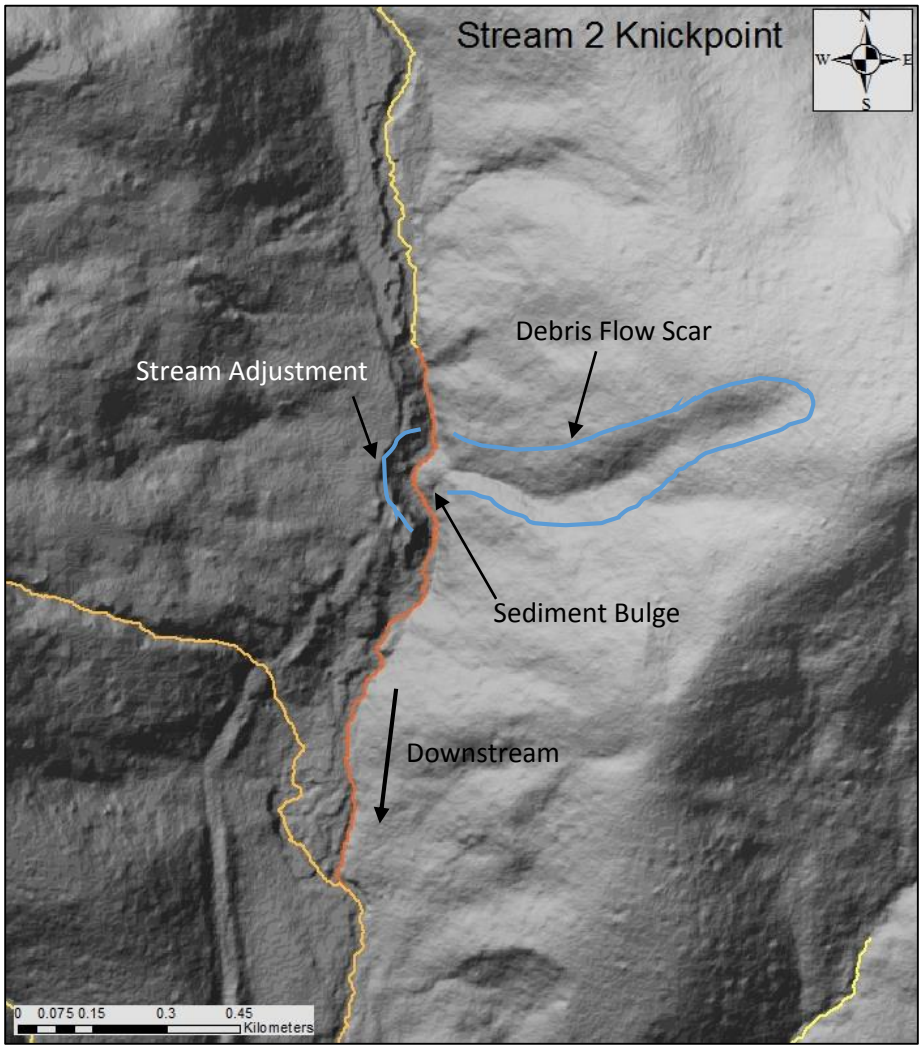

Figure 13. Along stream 2, within the Crescent Formation, there is an adjustment to the influx of material from a debris flow and shows up on the long profile as a knickpoint.

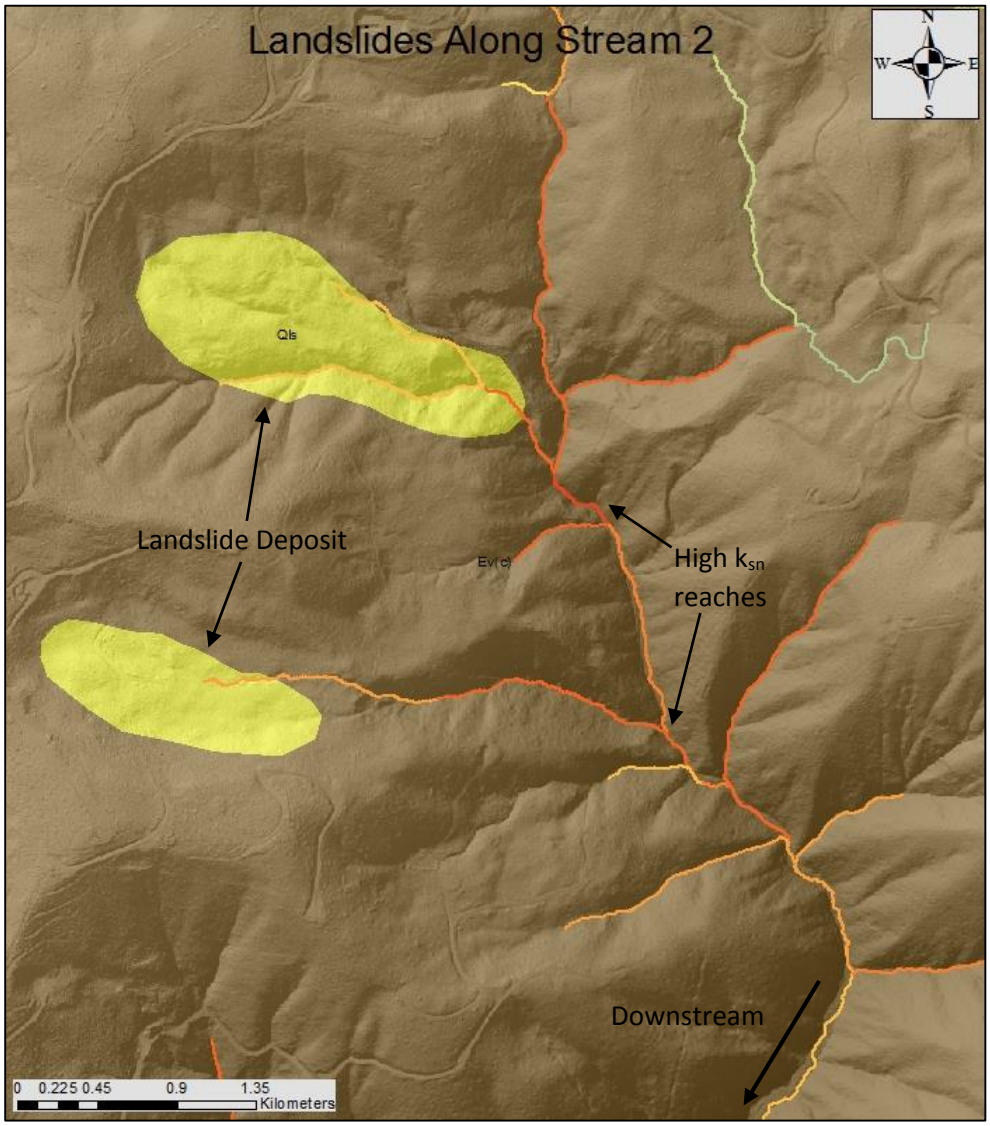

Figure 14. Near the headwater portions of stream 2, landslide deposits are feeding sediment into the channel and may be producing high ksn values.

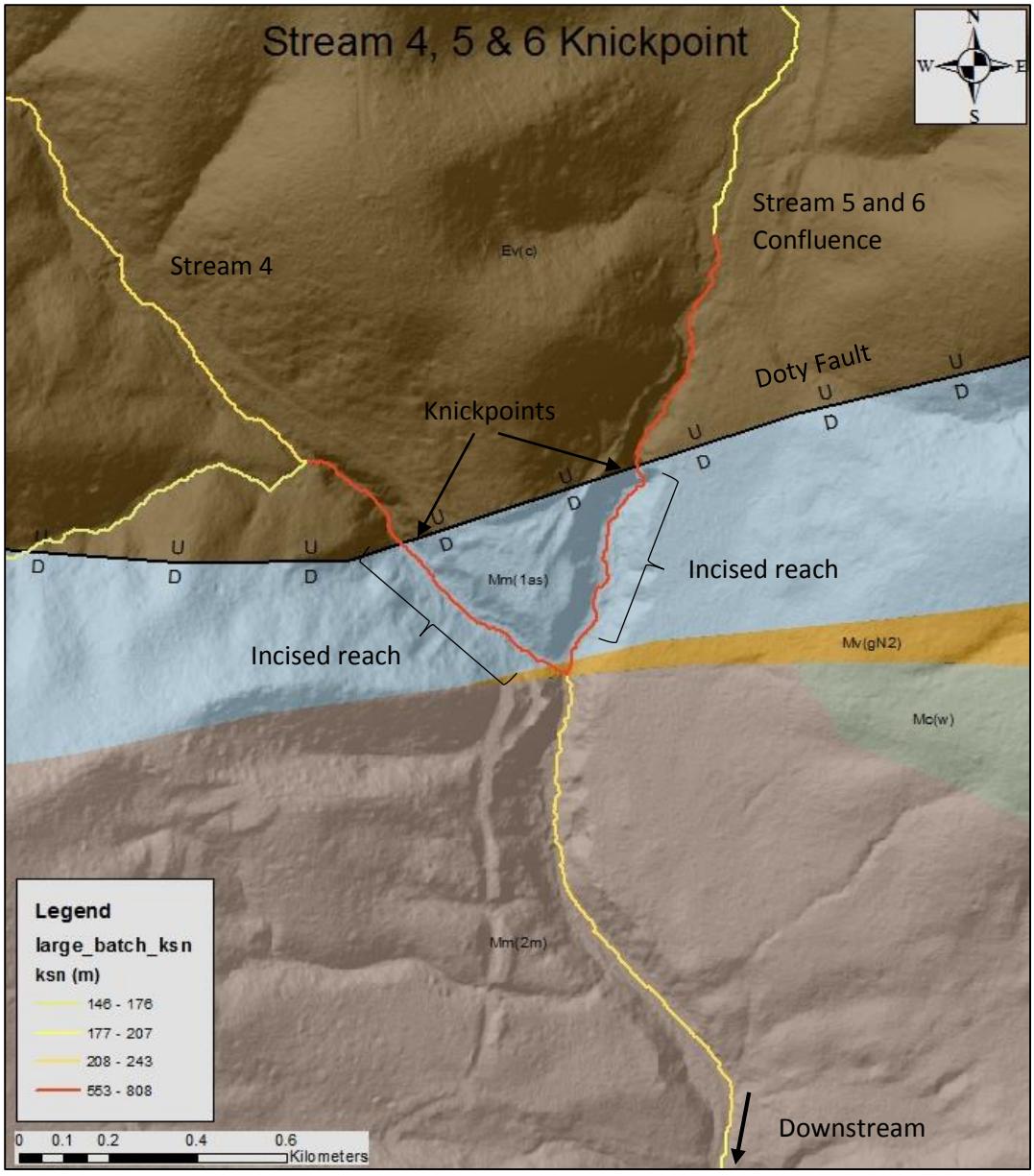

Figure 15. A combination of factors affects the morphology of Streams 4, 5 and 6. The Doty Fault, lithologic boundaries and stream confluences all may be influencing the location and size of the knickpoints. Geologic symbols: Ev(c) – Crescent Formation, Mm(1as) – Astoria Formation, Mv(gN2) – Grande Ronde Basalt, Mc(w) – Wilkes Formation, Mm(2m) – Montesano Formation.

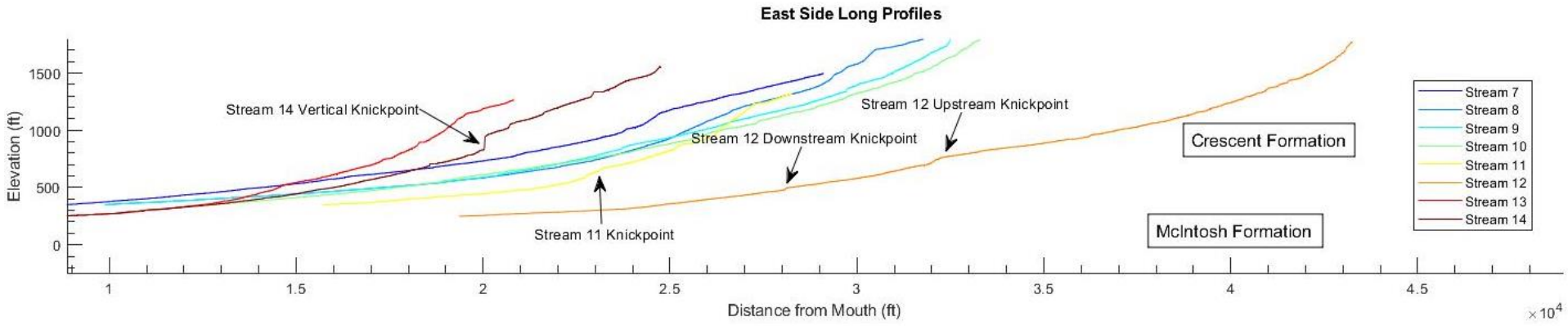

Figure 16. Composite diagram of east-directed stream profiles. Knickpoint locations are highlighted.

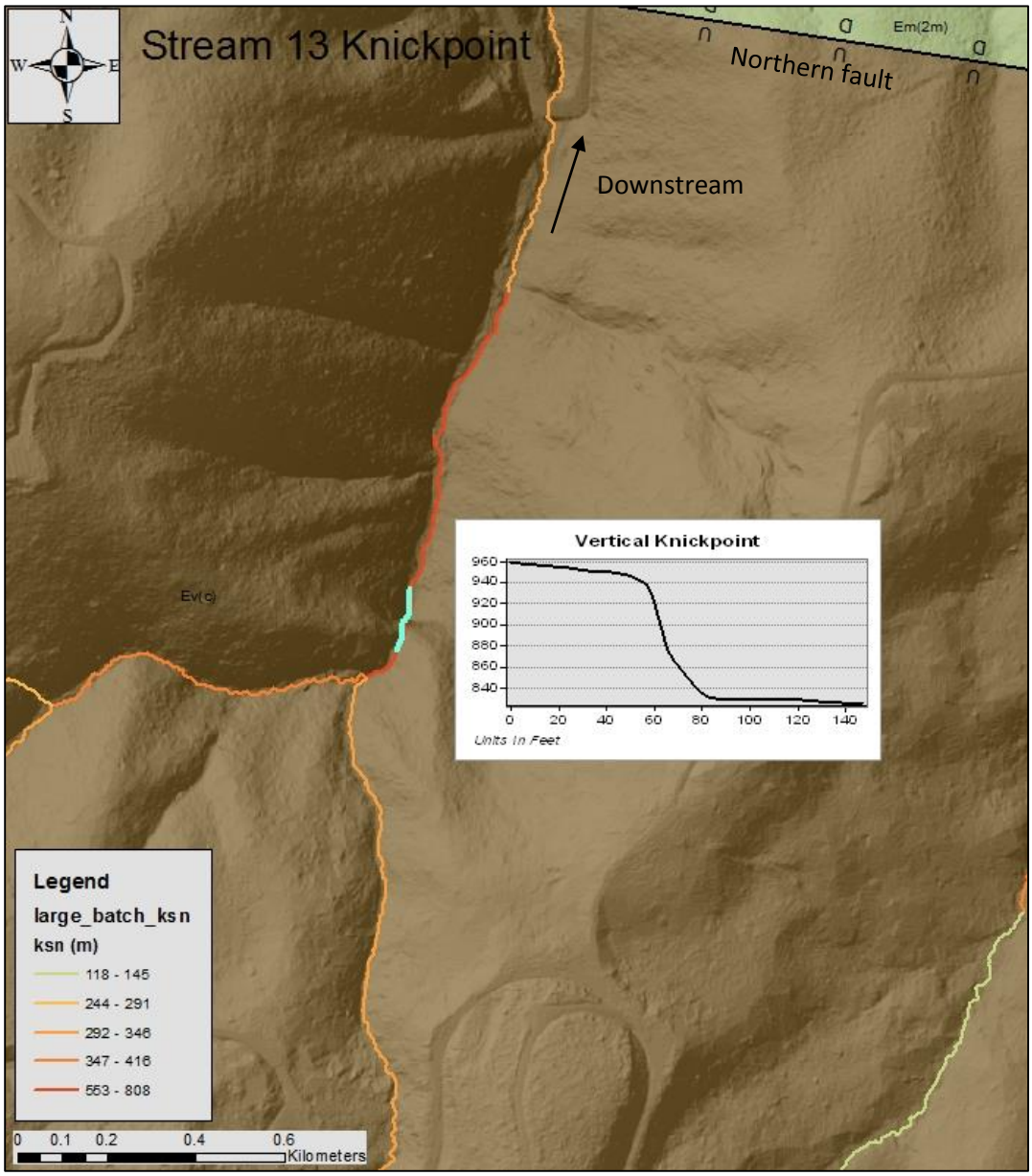

Figure 17. Vertical knickpoint along stream 13 within the Crescent Formation. Geologic Symbols: Ev(c) – Crescent Formation, Em(2m) – McIntosh Formation.

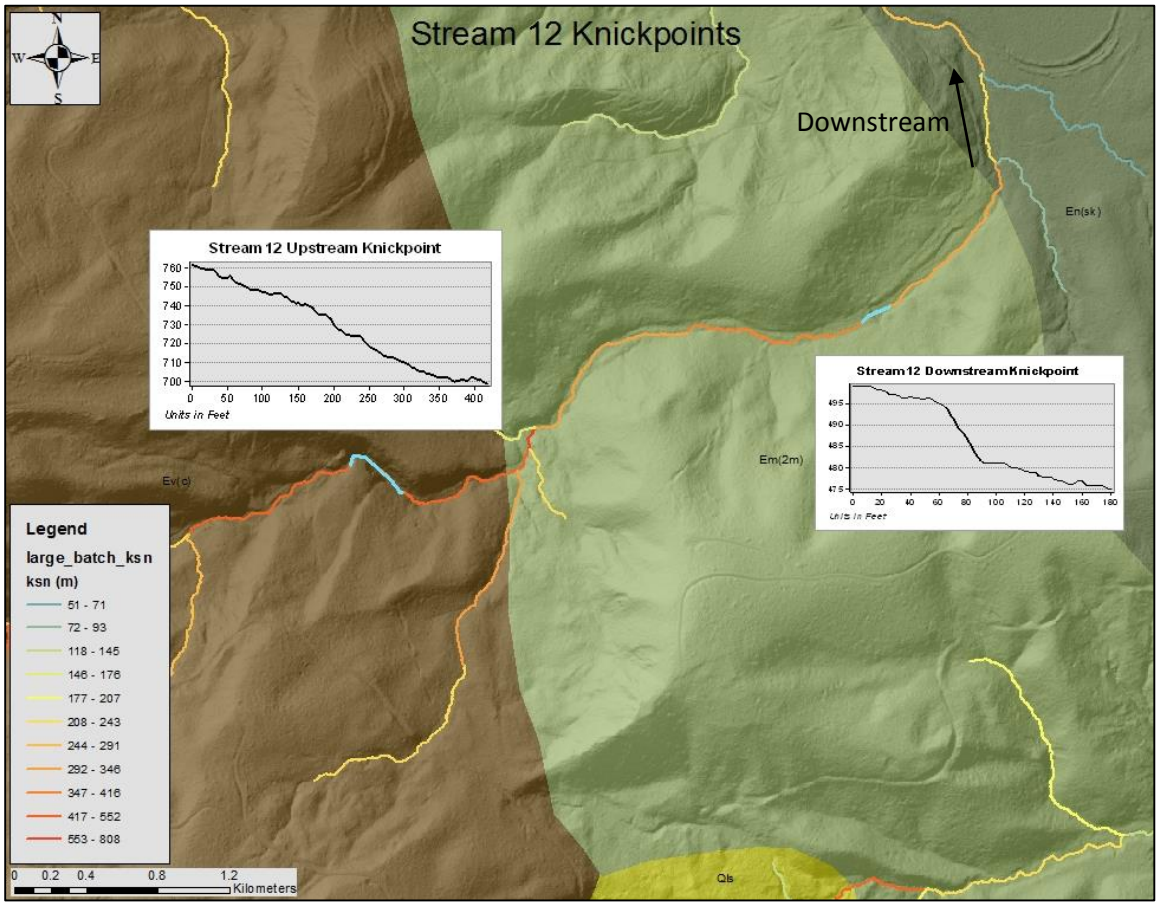

Figure 18. Two knickpoints located along stream 12. The upstream knickpoint is tied to a an incised area near the boundary of the Crescent and McIntosh Formations. The downstream knickpoint is isolated within the the McIntosh Formation. Geologic Symbols: Ev(c) – Crescent Formation, Em(2m) – McIntosh Formation, En(sk) – Skookumchuck Formation, Qls – Landslide Deposit.

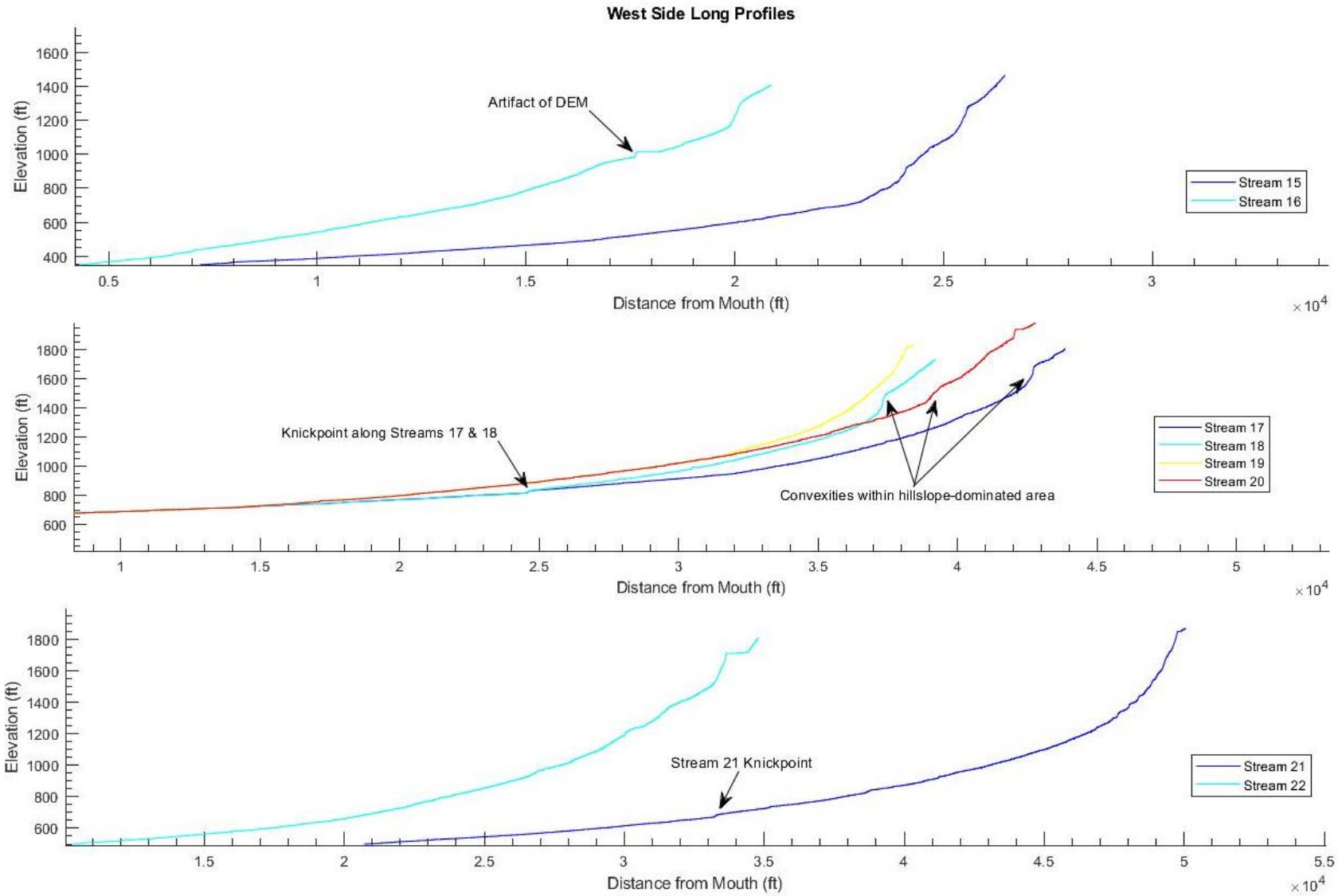

Figure 19. Composite diagrams of west-directed streams.

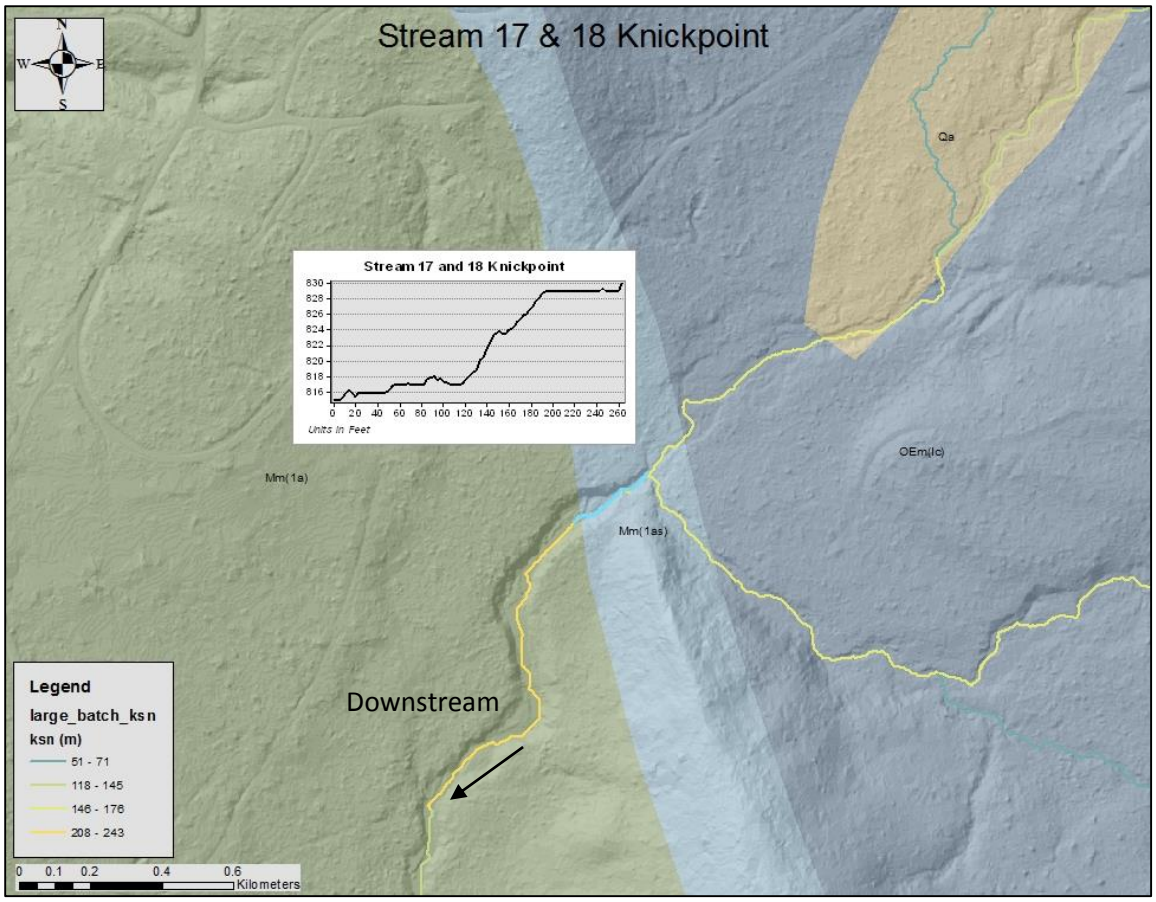

Figure 20. A knickpoint is located within the Astoria Formation – Saucesian Member, below the confluence of streams 17 and 18. Geologic Symbols: Mm(1a) – Astoria Formation, Mm(1as) – Astoria Formation (Saucesian), OEm(lc) – Lincoln Creek Formation, Qa – Quaternary alluvium.

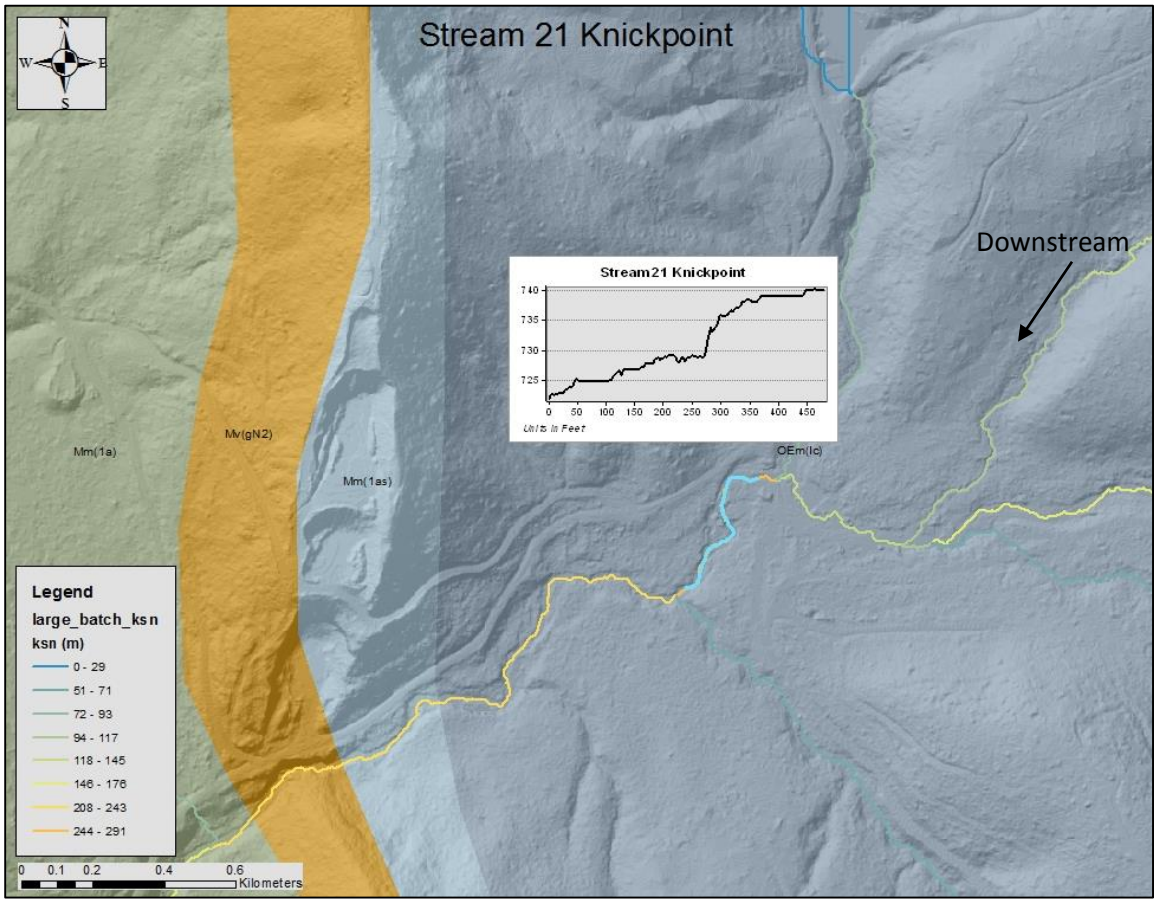

Figure 21. Knickpoint along stream 21 within the Lincoln Creek Formation. Alterations of the stream from logging and mining may create this change in stream gradient. Geologic Symbols: Mm(1a) – Astoria Formation, Mv(gN2) – Grande Ronde Basalt, Mm(1as) – Astoria Formation (Saucesian), OEm(lc) – Lincoln Creek Formation, Qa – Quaternary alluvium.

Appendix

Examples of MATLAB codes used in Topographic Analysis Toolkit (TAK):

```
[DEM,FD,A,S]=MakeStreams('D:\D--Temp\varqa\ArcGIS
10.5\Doty\doty_mosaic.txt',1e6,'resample_grid',true,'no_data_exp','DEM<=0')
```

```
KsnChiBatch(DEM,FD,A,S,'all',’ref_concavity’,0.5)
```

```
[knl,ksn_master,bnd_list,Sc]=KsnProfiler(DEM,FD,A,S,'input_method','interactive','pick_metho
d','stream','junction_method','ignore','concavity_method','ref','shape_name','doty_ksn','save_figur
es',true)
```

```
[Sc]=SegmentPicker(DEM,FD,A,S,i,'direction','down','min_elev',450,'plot_style','keep','ref_conc
avity',0.5)
```

```
ProcessRiverBasins(DEM,FD,S,RiverMouths,'calc_relief',false,'ref_concavity',0.5,'ksn_method',
quick,'write_arc_files',true)
```

```
SegmentPlotter(1,'label',true,'names',{'Stream1','Stream2',
'Stream3','Stream4','Stream5','Stream6'})
```